

# Co-movement and Lead–Lag Relationship Between Green Bonds and Renewable Energy Stock Markets: Fresh Evidence from the Wavelet-Based Approach

Nana Liu

China University of Mining and Technology - Xuzhou Campus: China University of Mining and Technology

Chuanzhe Liu (✉ [rdean@cumt.edu.cn](mailto:rdean@cumt.edu.cn))

China University of Mining and Technology <https://orcid.org/0000-0002-5911-1296>

---

## Research

**Keywords:** Green bonds, renewable energy markets, wavelet coherence, Causality, COVID-19

**Posted Date:** November 18th, 2020

**DOI:** <https://doi.org/10.21203/rs.3.rs-105937/v1>

**License:**  This work is licensed under a Creative Commons Attribution 4.0 International License.

[Read Full License](#)

---

1 **Co-movement and lead–lag relationship between green bonds and renewable energy**  
2 **stock markets: Fresh evidence from the wavelet-based approach**

3 Nana Liu <sup>1</sup>, Chuanzhe Liu <sup>1,\*</sup>

4 <sup>1</sup> School of Economics and Management, China University of Mining and Technology, Xuzhou 221116,  
5 China; liunana1004@cumt.edu.cn (N.L.);

6 \* Correspondence: rdean@cumt.edu.cn; Tel.: +86-516-83590168

7 **Abstract:**

8 **Background:** A recent study in *Nature Climate Change* shows that due to reduced human  
9 activities during the Coronavirus disease 2019 (COVID-19) pandemics, daily global  
10 emissions of carbon dioxide decreased by 17% from the average level in 2019. With the  
11 gradual recovery of economic activity and human energy consumption, the emissions of  
12 greenhouse gas and pollution would rise again. Green bonds are considered a crucial tool  
13 to release climate finance. The green bond market can act as an essential bridge between  
14 capital providers (i.e. institutional investors) and sustainable assets (i.e. renewable energy).  
15 This study is the first attempt to examine co-movement and the lead–lag relationship  
16 between green bonds and global and sector renewable energy stock markets in the time and  
17 frequency horizons. We apply continuous wavelet, wavelet coherence, and line and non-  
18 line causality approaches on data during the period 2010–2020, coincidentally including  
19 the COVID-19 pandemic.

20 **Results:** (1) Green bonds and renewable energy markets show evidence of a similar pattern  
21 based on the wavelet power spectrum, which shows high price volatility at small and  
22 medium scales, especially during periods of turbulence and crisis. (2) The dynamic  
23 connection between green bonds and renewable energy returns is weak (strong) on the short  
24 (long) time-scale. However, on medium-term time scales, the dependence between them is  
25 significant only during turbulent periods, such as the European Sovereign Debt Crisis 2012  
26 (ESDC) and the COVID-19 pandemic. (3) With regard to causality, our results show  
27 unidirectional and bidirectional linear (non-linear) causality at low and high frequencies.  
28 Moreover, our finding reveals the fact regarding the lead – lag relationship that, most of  
29 the time and frequencies, no one market necessarily dominates the other.

30 **Conclusion:** Our findings provide several remarkable policies and practical implications  
31 for market regulators and investors. Institutional investors can benefit by including green  
32 bonds in their portfolios to decrease their climate change risk and improve their  
33 environmental, social, and corporate governance rating in the portfolio. Considering that

34 the dependence between green bonds and renewable energy stock prices varies over various  
35 time scales, investors with different investment horizons should make diverse investment  
36 portfolio and hedging choices. The finding is also relevant for formulating green finance  
37 policies and supporting renewable energy investments. Policy decisions on the transition  
38 of energy to a decarbonized economy should consider the consequences for green bonds,  
39 which are also critical for the transition to a climate-resilient economy.

40 **Keywords:**

41 Green bonds; renewable energy markets; wavelet coherence; Causality; COVID-19  
42

43 **1. Background**

44 A recent study in *Nature Climate Change* [1] shows that due to reduced human activities  
45 during the Coronavirus disease 2019 (COVID-19) pandemics, daily global emissions of  
46 carbon dioxide decreased by 17% from the average level in 2019. Carbon emissions at the  
47 end of May 2020 were close to the level of 2006. With the gradual recovery of economic  
48 activity and human energy consumption, the emissions of greenhouse gas and pollution  
49 would rise again. To implement fully the *Paris Agreement 2015*, \$1.5 trillion in green  
50 financing would be required every year until 2030. Attracting low-carbon investment in  
51 green energy program has been a significant challenge and needs a major shift [2-4]. This  
52 shift requires government policy to reallocate financial resources, and one of the most  
53 effective ways to attract investment in more sustainable development projects is to promote  
54 green bonds [5].

55 Green bonds are considered a crucial tool to release climate finance [6, 7]. Green bonds  
56 are attracting increasing interest in Asia and around the world as an alternative source of  
57 financing for low-carbon projects [5, 8]. Green bonds are used differently compared with  
58 general bonds [9]. The green bond process is only used to finance the low-carbon projects,  
59 while general bonds are allowed to finance any legal project. Investors are well aware of  
60 the present challenges of climate change, and green bonds could fund our path to a more  
61 sustainable world [7]. The green bond market can act as an essential bridge between capital  
62 providers and sustainable assets. The green bond market has developed rapidly, growing  
63 from \$3.4 billion in 2012 to \$156 billion in 2017. To raise additional finance for clean  
64 production projects, the European Investment Bank and the World Bank were the first to  
65 issue green bonds in 2007 and 2008, respectively. The market is now gradually diversifying

66 in the types of issuer, geographic region and usage of funds. For example, 55 issuers from  
67 different countries/regions had issued green bonds by the end of 2019. International green  
68 bonds involve a total of 496 issuers, including multilateral development banks, sovereign  
69 countries, local governments, government-supported institutions, financial institutions, and  
70 non-financial enterprises [10].

71 Although the progress of green bond markets has been impressive, such markets still  
72 have opportunities for further growth and improvement [11]. The confirmed financing of  
73 green bonds occupies only 17% of the reported unlabeled climate-related bonds. To achieve  
74 further market growth, the coordinated action among many stakeholders is needed.  
75 Policymakers can help with the supply of green bonds (i.e. adopting cutting-edge climate-  
76 related green bond standards) and provide supportive policies to promote the growth of the  
77 renewable energy sector. Public capital providers could contribute to the elimination of  
78 renewable assets and support green bonds by providing seed capital, demonstration  
79 issuance and capacity building. Institutional investors may help by aligning their internal  
80 capabilities and investment objectives with long-term sustainability requirements. Other  
81 stakeholders, such as rating agencies, financial institutions, and retail investors, could also  
82 play an essential role in strengthening the green bond market and advancing global energy  
83 transition. Analyzing the risk spillover between green bonds and renewable energy markets  
84 on determining the market development of green bonds and their role in hedging portfolio  
85 risk is critical. Therefore, understanding how green bonds move with the stock prices of  
86 renewable energy is an essential concern for investors and policymakers.

87 To the best of our knowledge, this work is the first that focuses on the co-movement and  
88 lead-lag relationship between green bonds and renewable energy and considers the time  
89 and frequency scales simultaneously. Although wavelet analysis methods have been used  
90 in several studies on the connection between energy and financial asset returns[12-17] ,  
91 this study is the first attempt to analyze the interaction between green bonds and renewable  
92 energy using the continuous (discrete) wavelet transformation method. The primary  
93 advantage of the wavelet approach is that it allows us to distinguish short- and long-term  
94 investor behaviors. More precisely, market investors trade on a variety of time scales  
95 (expressed as frequencies) that range from seconds to years mainly because they have  
96 various degrees of beliefs, goals, preferences and institutional constraints, as well as  
97 distinct levels of information acceptance and risk tolerance. For example, agents with

98 shorter investment maturities, such as day traders or hedge funds, are more interested in  
99 the short-term actions of the market. Alternatively, other agents, such as large institutional  
100 investors, are more concerned with long-term market behavior. Therefore, an appropriate  
101 frequency band would help to understand better the co-movement of green bonds and  
102 renewable energy stocks at different frequency levels.

103 What should the relationship between the renewable energy stock prices and green bond  
104 yields be? There is a view that there should be a negative correlation using a present -value  
105 model. For instance, an increase in the discount rate in the future is expected to lead to a  
106 fall in share prices and an increase in long-term interest rates. However, there may also be  
107 a positive correlation, as changes in long-term interest rates may be related to information  
108 about the future dividend stream of the stock [18]. Several contradictory assumptions may  
109 predict a co-movement between these two green assets. This hypothesis is closely related  
110 to the theoretical arguments about the relationship between stock and conventional bonds  
111 [19], although the issuance of green bonds is ostensibly driven by the "green bond  
112 principle". There are the following representative hypotheses about risk spillovers between  
113 stock and bonds markets: (1) Financial risk contagion: In the absence of a material change  
114 in economic fundamentals, adverse shocks in one market are automatically transmitted to  
115 the other, leading to movements in the same direction, especially in times of extreme risk  
116 [20]; (2) Risk hedging needs: when the price of an asset deviates too much from its real  
117 value, hedgers will shift more of their positions to other safe assets to reach the target hedge  
118 ratio level [21]; (3) Asset substitution: Assuming that stocks and bonds are two perfectly  
119 competing assets, if the disclosure of relevant information helps increase the price of stocks,  
120 investors will be incentivized to convert bonds into stocks in their portfolio; if the  
121 information is more favorable to bonds, investors will replace their stock holdings with  
122 bonds [22]. When hypothesis (1) is confirmed, the stock and bond markets exhibit a  
123 "linkage effect"; when hypothesis (2) and hypothesis (3) are confirmed, there is usually a  
124 "seesaw effect" between the two. The co-movement between the two markets can also be  
125 explained by the above three hypotheses since the renewable energy stock and green bond  
126 markets are subordinate to the stock and bond markets, respectively. We expect financial  
127 contagion between the green bonds and renewable energy markets because, as an important  
128 source of funding for renewable energy companies, when the overall green bond market  
129 improves, investors expect the renewable energy markets to strengthen as well.

130 To this end, we analyze (i) dynamic co-movement and the lead–lag relationship between  
131 cross time-scale by applying cross-wavelet coherence and phase analysis, and (ii) the  
132 causality between green bonds and renewable energy returns by using (discrete) wavelet  
133 methods combined with linear and non-linear causality tests. We find that the interaction  
134 between green bonds and renewable energy returns is weak in the short time scale and that  
135 this weakness persists throughout the sampling period. In the long run (512 days-), green  
136 bonds are closely linked to the renewable energy market, despite differences between the  
137 global and sectoral indices. However, on medium-term time scales, the degree of  
138 dependence between these two markets is high only during turbulent periods. Concerning  
139 causality, our results show unidirectional and bidirectional linear (non-linear) causality at  
140 low and high frequencies. Moreover, our results reveal the fact regarding the lead–lag  
141 relationship that, at most time and frequency, no one market necessarily dominates the other.

142 This study investigates the idiosyncratic characteristics of return connections between  
143 green bonds and renewable energy markets. We examine these linkages because they are  
144 important for investment and risk management decisions. For example, portfolio managers  
145 often transfer funds from stocks to bonds when they expect stock market returns to decline.  
146 Reducing risk through this transfer depends on the linkages between the stock and bond  
147 markets. If cross-market asset returns are highly correlated, bonds would not provide the  
148 risk aversion that investors need. And if cross-market asset returns are negatively correlated,  
149 the possibility exists for long-term asset portfolios. Exploring the dynamics of the  
150 correlation between stock and bonds markets can provide theoretical support for the  
151 practice of asset allocation by institutional investors such as investment funds and  
152 insurance funds. Linkages between markets should also be taken into account when  
153 formulating regulatory policy, for example, market regulators would consider these  
154 linkages when assessing the effects of proposed policy changes.

155 This work provides a novel insight into green investment from a new perspective and  
156 contains at least four contributions on green bonds and renewable energy research. First,  
157 we use a continuous wavelet transformation method to distinguish between short- and long-  
158 term investor behavior in green bonds and renewable energy stocks. This aspect is  
159 important for investors who act at different time scales and over different periods. Indeed,  
160 from the perspective of portfolio diversification, green portfolio managers are more  
161 interested in higher frequency asset price linkages. In other words, they are concerned

162 about short-term movement. However, others are more interested in lower frequencies (i.e.,  
163 longer-term time scale). Second, using the frequency domain to understand the two main  
164 green assets better and choose the incentive policy that suits them is useful for  
165 policymakers. Third, a non-linear Granger causality model is applied to analyze further the  
166 relationship between green bonds and renewable energy over different time horizons.  
167 Fourth, we also use the most recent dataset, which happens to include the COVID-19  
168 epidemic period, resulting in extreme market volatility. As a result, we add an interesting  
169 period for the green bond and renewable energy markets.

170 The rest of the paper is organized as follows. Section 2 reviews the literature on green  
171 bonds and renewable energy. Section 3 introduces the data and reports a preliminary  
172 analysis. Section 4 outlines the methodology. Section 5 presents the empirical results.  
173 Section 6 offers primary conclusions and implications.

## 174 **2. Literature review**

175 Many researchers have focused on the relationship between green bonds and other  
176 markers. Pham [23] first provided evidence that the labelled green bond market is more  
177 volatile than the “unlabeled” bonds by using the Standard & Poor Co. (S&P) Green Bond  
178 Index. In a comparable study, Bachelet et al. [24] confirmed that green bonds issued by  
179 institutional issuers have higher liquidity than gray bonds. Reboredo [25] investigated the  
180 co-movement between green bonds and financial markets. This finding suggested a strong  
181 linkage between the treasury and corporate bond markets, and a weak connection between  
182 stock and energy commodity markets. Likewise, Reboredo and Ugolini [26] employed the  
183 value-at-risk (VaR) approach and discovered the price correlation between green bonds and  
184 financial markets. This study provided evidence that the green bond market is closely  
185 related to the fixed income and currency markets, resulting in a considerable price spillover  
186 effect and a negligible reverse effect. However, the green bonds market is weakly linked to  
187 these markets, such as stock, energy, and high-yield corporate bond markets. The research  
188 of Reboredo et al. [27] further provided a similar result to that of Reboredo and Ugolini  
189 [26] by using wavelet coherence methods; their finding suggested a strong connectedness  
190 between green bonds and treasury and corporate bonds over different time horizons and in  
191 the European Union (EU) and the United States (US); they found a weak linkage between  
192 green bonds and high-yield corporate bonds and stock and energy assets in the short and

193 long term. Recently, Jin et al. [28] made the first attempt to investigate the relationship  
194 between carbon futures and green bonds, as well as other three markets; this finding  
195 supported the evidence of the fact that the green bond market is the effective hedge for  
196 carbon futures and has performed well in periods of crisis. The relationship between green  
197 bonds and other markets could be affected by factors such as financial market volatility,  
198 economic policy uncertainty, oil prices, and positive and negative news reports on green  
199 bonds. Moreover, the attitudes and measures at all levels of governments can directly  
200 influence the green bond markets [29]. All of this prior literature invariably argued that the  
201 relationship between green bonds and energy was weak, with only considering the whole  
202 energy market, and failed to consider the renewable energy market.

203 It is noteworthy that the empirical relationship between green bonds and renewable  
204 energy has been considerably neglected. To the best of our knowledge, only a few articles  
205 provide an overview of the relationship between them[5, 8, 30] . For example, Liu et al.  
206 [32] investigated the dynamic dependence between green bonds and clean energy markets  
207 through a time-varying copula model. Hammoudeh et al. [33]analyzed the time-varying  
208 relationship between green bonds and other assets such as clean energy, CO2 emission  
209 allowance prices and other markets using a novel time-varying Granger causality test with  
210 July 30, 2014 to February 10, 2020 as the sample period. Nguyen et al. [34]consider the  
211 clean energy market in the study of the relationship between green bonds and other asset  
212 markets, and through the rolling window wavelet analysis method, the association between  
213 green bonds and clean energy is high, while the correlation with other markets such as  
214 stocks and commodities market is weak. Le, et al. [35] explore the return and volatility  
215 spillover effects between green bonds and financial technology and cryptocurrencies from  
216 both time domain and frequency domain perspectives, and the results show that green  
217 bonds can be used as good hedging assets.

218 Given that green bonds offer significant funding for renewable energy projects [31], the  
219 intrinsic connection between green bonds and the renewable energy market deserves  
220 further exploration. This study is the first attempt to examined the co-movement and lead–  
221 lag relationship between green bonds and renewable energy markets across different time  
222 horizons by applying (discrete) wavelet methods, and linear and non-linear causality tests.  
223 It would fill in the gaps for the empirical research of green bonds and renewable energy.

### 224 **3. Data**

225 We conduct an empirical analysis of co-movement and lead–lag relationship between  
226 green bonds and renewable energy stock prices on a range of time scale. In this case, we  
227 consider the daily data of three global and three sectoral renewable energy indices, as well  
228 as green bond indices. Referring to the research of Reboredo [36], we chose the S&P Dow  
229 Jones Green Bonds Index (hereafter GB) to indicate the global green bond market. Green  
230 bonds refer specifically to the bonds utilized to finance environmental projects. Given the  
231 diversity of the renewable energy market, it is crucial to consider different energy  
232 companies. Ugolini et al. [37] and Rezec and Scholtens [38] found a suitable basis for  
233 estimating the renewable energy market by targeting six indices for different sectors of  
234 renewable energy .

235 The three global indices include the following: (a) The Wilder Hill Clean Energy Index  
236 (ECO) is comprised of 42 companies focused on renewable energy technologies. The  
237 selection of stocks and sectors included in this index is based on their relevance to clean  
238 energy, technological advances, and the elimination of pollution [39, 40]. (b) The S&P  
239 500 Global Clean Index (GCE) is a weighted index comprised of more than 30 companies  
240 from around the world in the clean energy production or equipment industries, including  
241 clean energy production companies and equipment and technology companies [41]. (c)  
242 The European Renewable Energy Index (ERIX), which includes 30 of the largest European  
243 clean energy companies specifically involved with biomass, solar, geothermal, marine,  
244 water and wind energy [42]. The sectoral indices are as follows: (d) The ISE Global Wind  
245 Energy Index (WIND) is designed to track the performance of companies by offering listed  
246 products and services in the wind energy industry. (e) The MAC Global Solar Equity Index  
247 (SOLAR) is a diversified solar energy index that includes all solar energy technology,  
248 operations and financing across the value chain, and related solar equipment. (f) The S&P  
249 Renewable Energy and Clean Technology Index (TECH) measures the key performance of  
250 companies that focus on green technology and sustainable infrastructure solution.

251 The data for all indices are obtained from the Bloomberg database. Our sample period  
252 runs from March 29, 2010 to June 30, 2020 and totals 2670 daily observations, which  
253 coincidentally cover periods of major market turmoil, such as European Sovereign Debt  
254 Crisis 2012 (ESDC) and the COVID-19 period. We obtain the daily return series for all  
255 variables by the logarithmic difference method. Figure1 depicts the trend of fluctuations in  
256 a multi-pair time series, the trajectory of which may suggest a positive and strong

257 correlation between green bonds and renewable energies. Fig.2 reports the dynamics of  
258 green bond and renewable energy index returns. Interestingly, all indicators have a similar  
259 path, especially the energetic vibration during the ESDC crisis and the COVID-19  
260 pandemic, although the amplitude of the wave is different.

261

262

263

Insert Fig.1 here

264

265

Insert Fig.2 here

266

267 Table 1 reports the descriptive statistical characteristics of the returns on green bonds  
268 and six renewable energy assets. The mean values of the seven asset returns are all close  
269 to zero. The standard deviations indicate that the volatility of all return series except GB  
270 and SOLAR are similar. SOLAR returns have maximum and minimum extremes of 0.120  
271 and  $-0.15$ , respectively. Therefore, the risk of volatility is the highest. Conversely, a  
272 positive mean of GB has the smallest standard deviation (0.004) and is thus a safe  
273 investment. Moreover, this study finds that all variables are negatively skewed, with ECO  
274 and GCE having the highest negative skewness values ( $-0.75$ ) with the most obvious risk  
275 of collapse. At the same time, the excess peaks (higher than standard 3) indicate that all  
276 variables are characterized by a spiky thick-tailed distribution, which is also confirmed by  
277 the Jarque-Bera test. Ljung-Box and Autoregressive Conditional Heteroskedasticity-  
278 Lagrange Multiplier tests explicitly detect a correlation in the return series. The results of  
279 the unit root tests (i.e., ADF, PP and KPSS) reject the null hypothesis of the existence of a  
280 unit root at the 1% significance level, suggesting that all return series are stationary. Finally,  
281 Pearson correlation coefficients demonstrate that all renewable energy indices are  
282 positively correlated with green bond yields.

283

284

Insert Table 1 here

285

## 286 4. Methodology

### 287 4.1 Continuous wavelet transform (CWT)

288 The wavelet is a function constructed from a single wavelet known as the mother wavelet,

289 which is a real-valued squared productive function given by the following:

$$290 \quad \psi_{\tau,s}(t) = \frac{1}{\sqrt{s}} \psi\left(\frac{t-\tau}{s}\right), \quad (1)$$

291 where  $\frac{1}{\sqrt{s}}$  is the normalization constant that ensures the unit variance of the wavelet, and  
292  $\tau$  and  $s$  are the position and scale parameters that determine the precise position of the  
293 wavelet and wavelet expansion or stretching, respectively.

294 Each wavelet can help characterize different data. In this paper, we utilize Morlet  
295 wavelets, which are often used in the economic field, to obtain amplitude and phase. The  
296 Morlet wavelet consists of a Gaussian window Fourier transform in which the sine and  
297 cosine vibrate at the core frequency and is calculated as follows:

$$298 \quad \psi(t) = \pi^{-\frac{1}{4}} e^{iw_0 t} e^{-\frac{t^2}{2}}, \quad (2)$$

299 where  $\pi^{-\frac{1}{4}}$  is the standardized factor that ensures that the wavelet has a unit of energy,  
300  $e^{-\frac{t^2}{2}}$  as a Gaussian envelope with unit standard deviation, and  $e^{iw_0 t}$  denote a complicated  
301 sinusoidal curve. In the present study, we set  $w_0 = 6$  to represent the appropriate  
302 compromise between time and frequency localization.

303 The CWT  $W_x(s)$  is a useful tool that enables to analyze time evolution along with  
304 the frequency and is described as follows:

$$305 \quad W_x(s) = \int_{-\infty}^{\infty} x(t) \frac{1}{\sqrt{s}} \psi * \left(\frac{t}{s}\right), \quad (3)$$

307 where  $*$  denotes complex conjugation and the proportionality parameter  $s$  determines  
308 whether the wavelet can detect a higher or lower component of the sequence  $x(t)$ , which  
309 is possible when the tolerance condition is satisfied.

#### 310 4.2 Cross-wavelet power, wavelet coherence and phase differences

311 The application of continuous wavelet analysis in financial and economic fields is  
312 mainly focused on the multi-scale analysis of univariate variables. However, to examine  
313 the co-movement and lead-lag relationship between two variables in time-frequency  
314 domains simultaneously, cross-wavelet transform is also required.

315 The cross-wavelet transform explores the interdependence between green bonds  $x(t)$   
316 and renewable energy  $y(t)$  in a different frequency space, which can be formulated as  
317 follows:

$$318 \quad W_n^{XY}(\tau, s) = W_n^X(\tau, s) * W_n^Y(\tau, s), \quad (4)$$

319 where  $W_n^X(\tau, s)$  and  $W_n^Y(\tau, s)$  denote CWT of  $x(s)$  and  $y(s)$ , respectively and \*  
 320 represents the complex conjugate.

321 As opposed to the power wavelet, crossed wavelet power (XWP) represents the local  
 322 covariance in time and frequency for each sequence, and the formula is as follows:

$$323 \quad XWP^X(\tau, s) = |W_n^{XY}(\tau, s)|. \quad (5)$$

324 Wavelet coherence  $R_n^2(s)$  is also an important method for assessing the common  
 325 movement between green bonds and renewable energy in the time-frequency space. It  
 326 generates a quantity between 0 and 1 (a correlation coefficient), where 0 denotes a weak  
 327 inter-correlation and 1 means a strong interaction.  $R_n^2(s)$  is given by:

$$328 \quad R_n^2(s) = \frac{s^{-1}|W_n^{XY}(s)|^2}{(s^{-1}|W_n^X(s)|^2)(s^{-1}|W_n^Y(s)|^2)}, \quad (6)$$

329 where  $s$  is the smoothing element of time and scale. As suggested by Torrence and Compo  
 330 [43], Monte Carlo simulation methods can be used to perform statistical inference.

331 Moreover, whether the nexus between green bonds and renewables is positive or  
 332 negative and whether a lagging or lagging relationship exists can be measured by the phase  
 333 difference. Torrence and Webster [44] gave the following definition:

$$334 \quad \varphi_{xy}(s) = \tan^{-1} \left( \frac{\zeta(s^{-1}W_n^{XY}(s))}{\xi(s^{-1}W_n^{XY}(s))} \right), \quad (7)$$

335 where  $\zeta$  denotes the imaginary component and  $\xi$  represents the real part. When  
 336  $\varphi_{xy}(s) = 0$ , the two series are in the same period (in-phase), which implies that they are  
 337 positively interconnected. When  $\varphi_{xy}(s) = \pi$  or  $-\pi$ , the two series will be moved with  
 338 a  $180^\circ$  (out of phase), which suggests a negative association. Fig.3 provides a summary of  
 339 the different types of phases, represented by the direction and angle of the arrows.

340

341

Insert Fig.3 here

342

### 343 4.3 Discrete wavelet transform (DWT)

344 However, the CWT will create redundant information, which leads to inefficient analysis.  
 345 Therefore, the DWT is performed to account for specific time-frequency conditions  
 346 adequately.

347 Parameters  $s$  and  $\tau$  are discretized as  $s = 2^{-j}, \tau = 2^{-jk}, j, k \in Z$ , and the definition of  
 348 the wavelet function becomes the following:

349 
$$\psi_{j,k}(t) = 2^{\frac{j}{2}}\psi(2^j t - k), j, k \in Z. \quad (8)$$

350 Thus, the DWT is specified as follows:

351 
$$W_x(j, k) = \int x(t)\overline{\psi_{j,k}(t)}dt, j = 0,1,2, \dots, k \in Z. \quad (9)$$

352 A multi-resolution analysis is introduced to allow the decomposition of the return series  
353 into different scales. The decomposition of  $x(t)$  is calculated as follows:

354 
$$x(t) = \sum_k s_{j,k}\phi_{j,k}(t) + \sum_k d_{j,k}\psi_{j,k}(t) + \sum_k d_{j-1,k}\psi_{j-1,k}(t) + \dots + \sum_k d_{1,k}\psi_{1,k}(t), \quad (10)$$

355 where  $\phi$  and  $\psi$  are two fundamental functions referred to as father and mother wavelets,  
356 respectively, which describe the low and high-frequency section of the sequence. The  
357 parameters  $s_{j,k}$ ,  $d_{j,k}$ , ...,  $d_{1,k}$  are wavelet transform factors that determine the response  
358 of the corresponding wavelet function to the overall spectrum. Thus, using the J-level  
359 multiresolution decomposition analysis, the time series  $x(t)$  is represented as:

360 
$$x(t) = S_j(t) + D_j(t) + D_{j-1}(t) + \dots + D_1(t), \quad (11)$$

361 where  $S_j(t)$  is the base function or residual, and frequency components  $D_j(t)$  provides  
362 time-frequency details for the short, medium, or long term. In this study, we create eight  
363 separate multi-resolution levels based on sample data to filter the financial data  
364 appropriately and correctly (see Gençay et al., 2002,2005). The decomposition results in  
365 eight specific time-frequency include the following: (1) the highest frequency component,  
366 D1, indicates a time scale of 2 days (daily impact); (2) component D2 represents a time  
367 scale of 4 days (weekly impact); and (3) components D3, D4, D5, D6, D7, and D8 measure  
368 medium- and long-term variations from 8 days to 256 days.

#### 369 4.4 Linear and non-linear Granger causality tests

370 After converting the green bond and renewable energy variables into proportional  
371 components, we used the linear and non-linear Granger causality tests. Granger causality  
372 intends to examine whether the current and lagged values of a variable can significantly  
373 contribute to the prediction of the future value of another variable. The linear causality for  
374 two stationary series X and Y is calculated by a bivariate vector autoregressive (VAR):

375 
$$X_t = \alpha_0 + \sum_{i=1}^n \alpha_i X_{t-i} + \sum_{j=1}^q \beta_j Y_{t-j} + \varepsilon X, t, \quad (12)$$

376 
$$Y_t = \beta_0 + \sum_{i=1}^n \alpha_i X_{t-i} + \sum_{j=1}^q \beta_j Y_{t-j} + \varepsilon Y, t, \quad (13)$$

377 where X and Y are stable time series, and n and q are the lag lengths of X and Y, respectively.  
 378 The null hypothesis in the Granger causality test is that y does not cause x, which is  
 379 indicated by  $H_0: \beta_1 = \dots = \beta_q = 0$ . The contrast hypothesis is  $H_1: \beta_i \neq 0$  for at least one  
 380 j. The test statistic has a standard F distribution, in which the degrees of freedom are (n, T-  
 381 n-q-1) and T is the number of observations.

382 One weakness of linear causality measures is their failure to accommodate nonlinearities  
 383 in time series price dynamics [45-48]. Several authors have formulated a variety of  
 384 nonparametric tests for Granger's non-causal hypothesis. Baek and Brock [49] developed  
 385 a nonparametric statistical method based on correlation integration. Hiemstra and Jones  
 386 [50] introduced an adapted non-linear causality model that relaxes the assumptions of Baek  
 387 and Brock [49] about independent and identical distribution levels and mutual  
 388 independence. Furthermore, Diks and Panchenko [51] explored a new non-linear Granger  
 389 test, which is widely used to evaluate economic and energy market data. Thus, in the  
 390 present study, the non-linear Granger approach proposed by Diks and Panchenko [51] is  
 391 used to test the non-linear relationship between green bonds and the renewable energy  
 392 market.

393 Assuming two strictly stationary time series  $X_t$  and  $Y_t$ , if the past and current values  
 394 of  $X_t$  contain additional information about the future value of Y that is not included in the  
 395 past and current  $Y_t$  values, then  $X_t$  strictly Granger leads to  $Y_t$ .  $F_{X,t}$  and  $F_{Y,t}$  denote the  
 396 set of past information for  $X_t$  and  $Y_t$  before time t + 1, respectively, and order  $\sim$  indicates  
 397 the equivalent distribution. The time series  $X_t$  is the Granger causality of  $Y_t$  when the  
 398 following conditions are met:

$$399 \quad (Y_{t+1}, \dots, Y_{t+k}) | (F_{X,t}, F_{Y,t}) \sim (Y_{t+1}, \dots, Y_{t+k}) | F_{X,t}, \quad (14)$$

400 where  $k \geq 1$  is the forecast border. Given the lag vectors  $X_t^{L_x} = (X_{t-L_x+1}, \dots, X_t)$  and  
 401  $Y_t^{L_y} = (Y_{t-L_y+1}, \dots, Y_t)$ , ( $L_x, L_y \geq 1$ ), the null hypothesis supposes that the past  
 402 observations of  $X_t^{L_x}$  include no additional information about  $Y(t+1)$  compared with  
 403 those of  $Y_t^{L_y}$ .

$$405 \quad H_0: Y(t+1) | (X_t^{L_x}, Y_t^{L_y}) \sim Y(t+1) | Y_t^{L_y}. \quad (15)$$

406 For the strictly stationary time series, Eq. 15 follows the invariant distribution of the  $(L_x +$   
 407  $L_y + 1)$ - dimensional vector  $W_t = (X_t^{L_x}, Y_t^{L_y}, Z_t)$ , where  $Z_t = Y_{t+1}$ . To keep the  
 408 following presentation and discuss denote ion compact, we dropped the time subscript and

409 assume  $L_x = L_y = 1$ . The conditional distribution of  $Z$ , given  $(X, Y) = (x, y)$ , was assumed  
 410 to be the same as that of  $Z$  given  $Y = y$ . Thus, we redefined the Eq.14 as follows:

411

$$412 \quad \frac{f_{X,Y,Z}(x, y, z)}{f_Y(y)} = \frac{f_{X,Y}(x, y)}{f_Y(y)} \cdot \frac{f_{Y,Z}(y, z)}{f_Y(y)}. \quad (16)$$

413

414 Following Eq. 16, for each fixed value of  $y$ ,  $X$  and  $Z$  are conditionally independent of  $Y$   
 415  $= y$ . Thus, the modified null hypothesis indicates that the following equation is satisfied:

$$416 \quad q \equiv E[f_{X,Y,Z}(x, y, z)f_Y(y) - f_{Y,Z}(y, z)] = 0. \quad (17)$$

417 Let  $\hat{f}_W(W_i)$  as the local density estimator of the random vector  $W$  at  $W_i$ ,

418

$$419 \quad \hat{f}_W(W_i) = \frac{(2\varepsilon_n)^{-d_W}}{(n-1)} \sum_{j, j \neq i} I_{ij}^W, \quad (18)$$

420 where  $I_{ij}^W = I(\|W_i - W_j\| < \varepsilon_n)$ ,  $I(\cdot)$  represents the indicator function, and  $\varepsilon_n$  stands  
 421 for the bandwidth parameter related to the  $N$  number of samples. Given an estimate of the  
 422 local density function, the following test statistics is constructed:

$$423 \quad T_n(\varepsilon_n) = \frac{n-1}{n(n-2)} \cdot \sum_i \left( \hat{f}_{X,Y,Z}(X_i, Y_i, Z_i) \hat{f}_Y(Y_i) - \hat{f}_{X,Y}(X_i, Y_i) \hat{f}_{Y,Z}(Y_i, Z_i) \right). \quad (19)$$

424 For  $L_x = L_y = 1$ , when  $\varepsilon_n = Cn^{-\beta}$  ( $C > 0, \frac{1}{4} < \beta < \frac{1}{3}$ ), the statistic  $T_n(\varepsilon_n)$  satisfies  
 425 the following conditions:

$$426 \quad \sqrt{n} \frac{(T_n(\varepsilon_n) - q)}{S_n} \xrightarrow{D} N(0,1), \quad (20)$$

427 where  $\rightarrow D$  is the convergence of the distribution and  $S_n$  stands for the estimate of the  
 428 asymptotic variance of  $T_n(\cdot)$ .

## 429 5. Results and discussion

### 430 5.1. Evidence from continuous wavelet analysis

431 The unconditional correlations (see the last row of Table 1) provide proof that green  
 432 bonds are correlated with renewable energy. This study spans a long period. Thus,  
 433 understanding how these correlations develop over time and explore whether dependency  
 434 varies with frequencies (i.e., whether more distinctive interdependencies exist over longer  
 435 or shorter investment horizons) would be interesting. The wavelet coherence method  
 436 allows us to investigate the correlations in time and frequency fields simultaneously.

437 Figure 3 displays the CWT power spectrum of the green bond and renewable energy  
 438 return series. The horizontal axis represents time, and the vertical axis stands for the  
 439 frequencies, which are converted to units of time (day) for ease of interpretation. In terms

440 of technology, as in previous related studies [13, 52, 53], we used Monte Carlo simulations  
441 to assess statistical significance. The bold black contour represents the regions that are  
442 significant at the 5% level. The black line of the curve indicates the cone of influence (i.e.,  
443 the area affected by the edge effect). The warmer (cooler) color represents the more intense  
444 (smooth) fluctuations in the time-frequency domain.

445 First, the results of the wavelet power spectrum may help us identify common islands  
446 between the green bond yield and the renewable energy return index on different time  
447 horizons. Closely inspecting Fig.4, the green bonds and renewable energy show a  
448 significant power in the same period and frequency from 2010 to 2012 and early 2020 on  
449 the scale of 1 day to 256 days. Therefore, these markets show evidence of the same pattern  
450 based on the wavelet power spectrum. The wavelet power spectra show high price volatility  
451 at small and medium scales, especially during periods of turbulence and crisis, such as the  
452 2012 ESDC, the Fed's interest rate hike policy in 2016, and the recent COVID-19 pandemic.  
453 This finding may suggest that the relationship between the green bond market and  
454 renewables is much solid during the period of crisis.

455 Moreover, the high-power region is also apparent in Fig. 4 at the lowest scales (1-day  
456 scale to 32-day scale) for all the renewable energy markets over the entire research period.  
457 This observation reveals that a significant period of price volatility in the renewable energy  
458 markets exists at low scales, which may be attributed to the anxiety of investors and market  
459 traders to intervene in these markets in the short term. The mix of cool and warm colors  
460 across the graph shows no clear evidence of structural change in the series.

461 Furthermore, the wavelet power spectrum plot shows, in the upper left (early 2010 to  
462 2012) and top right corner (early 2020) of the wavelet power spectrum for green bond  
463 returns, obvious red and yellow islands, indicating high power. However, in other regions,  
464 in short-, medium-, and long-term scales, the plot shows intense blue islands (deficient  
465 power). This finding may demonstrate that, except for the crisis periods, the price of green  
466 bonds showed stable fluctuations.

467

468

Insert Fig.4 here

469

470 The cross-wavelet power is applied to calculate the wavelet coherence coefficients for  
471 the local covariance between the green bond and renewable energy markets at various times

472 and frequencies. The wavelet coherence diagram (Fig. 6) visually displays the strength of  
473 the local relation between the green bonds and the renewable energy market in the time-  
474 frequency space. It can also reveal the leading-lagging relationship (correlation) of the  
475 phase-difference information between the two. The arrow pointing in the right direction  
476 indicates that the two are in phase, that is, they are positively correlated and vice versa. The  
477 arrow pointing up means the green bond is ahead of the renewables and vice versa.

478 Fig. 5 displays the results of the cross-wavelet transformation between green bonds and  
479 renewables, showing the local association between these indicators at different times and  
480 frequencies. The cross-wavelet correlation characteristics between green bonds and the six  
481 renewable energy sources are similar. Moreover, the evidence in Fig. 5 also suggests that  
482 the covariance is gradually weakening as the frequency decreases, which means that the  
483 correlation between green bonds and renewable energy returns is more affected by short-  
484 term shocks than by long-term and sustained changes. When cross wavelet coherence is  
485 particularly high, specific periods (2010–2012 and early 2020) and particular frequencies  
486 (high) can be identified. Furthermore, the impact strength of green bonds on renewable  
487 energies decreases over time such that, in the following years of the sample (2017–2019),  
488 covariance decreases across all time horizons and all variables. In addition, the available  
489 information on the phases (indicated by the arrows) suggests that the association between  
490 green bonds and renewable energies is not uniform across time scales because the arrows  
491 point upwards, to the right, and to the left on different time scales.

492

493

Insert Fig.5 here

494

495 Moreover, the wavelet coherence and phase difference are applied to detect the lead-lag  
496 relationship of green bond-renewable energy pairs. In the wavelet coherence diagram (Fig.  
497 6), the color grade orders from warmer (higher cohesion) to cooler (lower cohesion). The  
498 lowest coherence is close to 0 (dark blue), implying a perfect negative cohesion, whereas  
499 the highest cohesion is close to +1 (dark red), which means a perfect positive cohesion.  
500 The horizontal axis shows time, and the vertical represents the period, converting it to units  
501 of time (days).

502 The visual inspection of Fig. 6 reveals several interesting findings. We have identified  
503 that these markets share the same pattern over the long-term horizon. Green bond and

504 renewables are weakly reliant at high frequencies, and this weakness persists throughout  
505 the entire sampling period. However, green bonds have become less dependent (fewer red  
506 islands) on the renewable energy market after 2012. In the short-term, the correlation  
507 between green bonds and renewable energies is time-varying. As a result, the coherence is  
508 unstable with time (a few continuous red or blue islands). However, at lower frequencies  
509 (512 days-), a persistent red area is seen at the lowest bottom of the wavelet correlation  
510 plot, except for TECH, where the long-term scale relationship weakens, suggesting that  
511 green bonds are strongly correlated with the renewable energy market (only except for  
512 TECH). Fig. 6 also shows that the red islands increased massively on intermediate time  
513 scales during the 2010–2012 crisis and the COVID-19 pandemic, suggesting that the  
514 connection between the green bonds and the renewable energy indices is only highly  
515 dependent on the medium scale during the turmoil. This strong link between green bonds  
516 and renewables during the crisis can be explained by the following fact: the fundamentals  
517 of common action behavior (medium and long-term investors) are compromised during the  
518 whole non-calm period.

519 Furthermore, we also observe that the phase shown by the arrows in Fig. 6 is pointing to  
520 the right most of the time and frequencies, suggesting that the local relevance is positive  
521 and that renewables do not dominate the price of green bonds. The low frequency (512  
522 days-) of all pairs shows that the global renewable energy indices (i.e., ECO and GCE) and  
523 the sector renewables (i.e., WIND) have changed from pointing to the upper right to the  
524 right since 2013, which provides some rough and brief evidence that, early in the sample,  
525 green bonds are ahead of changes in renewable energy prices. However, as time evolves, a  
526 positive correlation and no lead–lag relationship are observed between the two. For the  
527 ERIX index, the phase points to the upper right on the low-frequency (512-day-) scale,  
528 indicating that green bond prices are leading the renewable energy prices. This evidence is  
529 consistent throughout the sample period. However, for the sectoral renewable energy index  
530 (i.e., SOLAR and TECH), at the low frequency (512 days-), the arrows point mainly to the  
531 lower right, which shows that green bond prices are lagging renewable energy prices. Our  
532 empirical results provide new evidence for co-movement between green bond and  
533 renewables.

534

535

Insert Fig.6 here

536

## 537 5.2. Evidence on causality

### 538 5.2.1 Linear Granger causality analysis between green bonds and renewable energy 539 markets

540 In the linear Granger causality test, a bivariate VAR model of the market is developed,  
541 and the Akaike information criterion (AIC) criterion is used to determine the optimal lag  
542 order. Tables 2 and 3 show the results of the linear Granger causality test between the green  
543 bond market and the renewable energy market for the original and decomposed data,  
544 respectively. For the original returns series, the empirical results demonstrate bidirectional  
545 linear Granger causality between the green bonds and renewable energy market at the 5%  
546 significance level, except for CEO and SOLAR, which have unidirectional linear Granger  
547 causality from green bonds to the renewable energy markets. Although renewable energies  
548 are based on supply and demand of the market, green bond prices still have an important  
549 effect on renewable energy markets.

550 On multiple time scales, the green bonds and renewable energy markets display different  
551 linear Granger causality. For the short-term (D1), the linear Granger non-causality is  
552 rejected at the 5% significance, indicating unidirectional linear Granger causality running  
553 from the renewable energy market to the green bond market. It also shows that the volatility  
554 of renewable energy prices in the short term has a linear effect on the green bond market.  
555 Nonetheless, for the ERIX and TECH markets, which are exceptions, we do not find linear  
556 causality between green bonds and TECH on short-run time scales.

557 However, on medium time scales D2–D7 (more than one week and less than one year,  
558 excluding non-working days), the linear Granger test results support that, in most cases,  
559 the two markets are linearly correlated at the 5% significance level. Using the linear  
560 Granger causality test, bidirectional Granger causality is observed between green bonds  
561 and renewable energy markets for most modes on intermedium time scales (i.e., D2, D3,  
562 and D4), as well as unidirectional Granger causality running from the green bond market  
563 to renewable energy market for D6. Moreover, for D7, a linear Granger relationship is not  
564 found in these two markets, except for ERIX and WIND. These results have two possible  
565 reasons. First, the formation of D2–D6 is influenced by factors with medium-term  
566 implications, such as shocks from major episodes or structural alterations in renewable

567 energy policy that could alter the whole renewable energy system and lead to comparable  
568 market changes, thereby increasing spillovers between green bonds and renewable energy  
569 markets. Second, due to the long duration of the volatility, eliminating the impact of these  
570 factors on market shocks in the short term is difficult, and the impact can spread from one  
571 market to the other. Overall, over the medium-term horizon, a significant bidirectional  
572 linear Granger is observed between the green bonds and the renewable energy market. As  
573 for the long-run trends, linear Granger causality tests suggest that the two return series are  
574 expected to increase in approximately 216 days (i.e., almost one year, excluding non-  
575 working days) over a reasonably long time horizon in both directions. Therefore, despite  
576 their distinctive characteristics, the long-term trends in both market returns follow similar  
577 patterns, slowly fluctuating around the zero mean.

578

579

580

581

582

583 5.2.2 Non-linear Granger causality between green bonds and renewable energy  
584 markets

585 The non-linear Granger causality tests use non-linear models to detect the non-  
586 linear relationship between the green bonds and renewable energy markets at original and  
587 decomposition data. Table 5 gives the values of the statistics  $T$  and  $P$ . According to the  
588 research of Diks and Panchenko [51], the parameter  $C$  of the bandwidth is 8, and the  
589 theoretical optimal rate of  $\beta$  is  $2/7$ , and with reference to Yu et al. [54], we set the optimal  
590 bandwidth  $\varepsilon_n$  to 1.5 based on our sample size.

591 For the original data, we discovered that the Granger causality was rejected at a 5%  
592 significance level on the return sequence, that is, bidirectional non-linear Granger causality  
593 is observed between the green bonds and the renewable energy market. This observation is  
594 different from the unidirectional linear Granger relationship running from the renewable  
595 energies (i.e., ECO and SOLAR) to the green bond market. For short-term time scales, the  
596 non-linear Granger non-causality between green bonds and renewable energy markets is  
597 rejected at a 5% significance level, indicating bidirectional non-linear Granger causality  
598 between the two markets. The short-term fluctuations of the green bond and the renewable

599 energy markets have a non-linear interaction with each other. This finding is different from  
600 the linear Granger causality test, which only found that most of the short-term fluctuations  
601 in the renewable energy market would affect the short-term fluctuations in the green bond  
602 market.

603 For intermediate time scales (i.e., more than one week and less than one year, excluding  
604 non-working days), the Granger test results find evidence supporting a non-linear  
605 relationship between the two markets in most cases, with a significance level of 5% (see  
606 Panel B-G of Table 5). For the majority of cases, the results of the non-linear Granger  
607 causality test are consistent with that of the linear Granger causality test. Nonetheless, some  
608 discrepancies remain between the linear and non-linear test results. For instance, non-linear  
609 bidirectional Granger causality at D5 and D6 can be statistically demonstrated at the 5%  
610 significance level, but we do not identify linear causality running from the green bonds to  
611 the renewable energy market. The possible reasons are the drivers of these patterns on  
612 intermediate time scales (i.e., major events and policy changes, which are well-documented)  
613 can lead to structural breakdowns in the renewable energy market. Given this structural  
614 fracture, the two return series exhibit visible non-linear characteristics on the medium time  
615 scales, and the traditional linear Granger causality model may be difficult to capture. On  
616 the contrary, the bidirectional Granger relationship on the medium-term can be effectively  
617 examined by the non-linear Granger causality test.

618 Focusing on the long term D8 (i.e., more than one year, excluding non-working days),  
619 the test findings support the evidence of non-linear Granger causality between the two  
620 return series (See Panel H in Table 5). This result is quite different from the linear Granger  
621 causality test, which identifies the linear bidirectional Granger causality over a long period.  
622 The primary explanation could be attributed to the simple, linear, and low-level complexity  
623 characteristic of the two long-term market trends. Given that the two series move slowly  
624 on a smooth curve without significant structural breaks, the connection mechanism  
625 between them may be following a simple linear relationship rather than a complex non-  
626 linear relationship. In general, our findings reveal that the green bond market is closely  
627 associated with the renewable energy market.

628  
629  
630

Insert Table 4 here
Insert Table 5 here

631

## 632 **6.Conclusion and implications**

633 Assessing the co-movement between green bonds and renewable energy markets has  
634 become one of the most pioneering and interesting topics to elaborate on the potential  
635 benefits of green bonds portfolio diversification and risk management. In this study, we  
636 provided fresh evidence for the time-frequency dynamic co-movement and lead-lag  
637 relationship between green bonds and six renewable energy markets from March 29, 2010  
638 to June 30, 2020 by using (discrete) wavelet analysis, wavelet coherency, cross wavelet  
639 methods, and linear and non-linear causality tests. Several important pieces of evidence  
640 can be concluded as follows.

641 Green bonds and renewable energy markets show evidence of a similar pattern based on  
642 the wavelet power spectrum, which shows high price volatility at small and medium scales,  
643 especially during periods of turbulence and crisis. The wavelet coherence analysis, which  
644 shows that the common movement between the pair of return sequences depends on time  
645 and frequency, is greatly impacted by the financial crisis, which cannot be captured by  
646 traditional time series techniques. We provided evidence that the dynamic interaction  
647 between green bonds and renewable energy returns is weak in the short-term and that this  
648 weakness persists throughout the sampling period although green bonds have become less  
649 dependent (fewer red islands) on the renewable energy market after 2012. In the long time  
650 scale (512 days-), green bonds are strongly correlated with the renewable energy market  
651 despite slight differences between the global and sectoral indices. However, on medium-  
652 term time scales, the connection between the green bond market and the renewable energy  
653 market is highly dependent only during turbulent periods, such as the 2010–2012 ESDC  
654 and the COVID-19 pandemic. With regard to causality, our results show unidirectional and  
655 bidirectional linear (non-linear) causality at low and high frequencies. Moreover, our  
656 finding reveals the fact regarding the lead - lag relationship that, most of the time and  
657 frequencies, no one market necessarily dominates the other.

658 Our findings provide several remarkable policies and practical implications for market  
659 regulators and investors. Specifically, the fact that the price of green bonds is less volatile  
660 than that of renewable energy stocks provides a new investment target for investors.  
661 Investors consider green bonds as investment assets and/or hedge portfolio risk while  
662 holding investment positions in energy stock assets. Institutional investors can also benefit

663 more by including green bonds in their portfolios because doing so would decrease their  
664 climate change risk and improve their environmental, social, and corporate governance  
665 rating in the portfolio.

666 Considering that the dependence between green bonds and renewable energy stock  
667 prices varies over various time scales, investors with different investment horizons should  
668 make diverse investment portfolio and hedging choices. Our evidence shows that green  
669 bonds and renewable energy assets are weakly correlated in the short run. Therefore, short-  
670 term investors could use green bonds as a hedge against renewable energy investments to  
671 reduce risk volatility. On the medium-term scale, given that the relationship would further  
672 strengthen during turbulent periods, investors should focus on the risk transfer between the  
673 two markets and design appropriate portfolio ratios to reduce and diversify portfolio risk.

674 We found evidence that green bonds and clean energy markets are positively correlated  
675 and co-moved on long time scales. Moreover, the results of the Granger test indicate  
676 bidirectional Granger causality between green bonds and renewable energy stocks, which  
677 prevents investors from taking advantage of hedging. However, investors could design  
678 their portfolios using the evidence of linear and non-linear causality because these two  
679 markets would use each other for useful information in determining their future values.  
680 Particularly, information from other markets should be carefully considered when  
681 forecasting market prices for green bonds or renewable energy.

682 Our finding is also relevant for formulating green finance policies and supporting  
683 renewable energy investments. In particular, when renewable energy and green bond prices  
684 move up (down) together, public clean energy funding can have an impact on renewable  
685 energy companies. This influence may result in a price externality for green bonds.  
686 Likewise, the removal of supportive policies (e.g., subsidies) for renewable energy would  
687 negatively affect the price of renewable energy stocks, which may transmit to the price of  
688 green bond assets. Therefore, policy decisions on the transition of energy to a decarbonized  
689 economy should consider the consequences for green bonds, which are also critical for the  
690 transition to a climate-resilient economy.

691 For future work, we would further combine the wavelet correlation and dynamic hedging  
692 models to examine the dynamic correlation and volatility spillover between green bonds  
693 and renewable energy returns to help hold optimal portfolio weights and hedge ratios  
694 especially in times of crisis and under different market conditions.

695 **Abbreviations:**  
696 COVID-19: The Coronavirus disease 2019  
697 ESDC: The European Sovereign Debt Crisis 2012  
698 S&P: The Standard & Poor Co.  
699 VaR: value-at-risk  
700 EU: The European Union  
701 US: The United States  
702 GB: The S&P Dow Jones Green Bonds Index  
703 RE: renewable energy  
704 ECO: The Wilder Hill Clean Energy Index  
705 GCE: The S&P 500 Global Clean Index  
706 ERIX: The European Renewable Energy Index  
707 WIND: The ISE Global Wind Energy Index  
708 SOLAR: The MAC Global Solar Equity Index  
709 TECH: The S&P Renewable Energy and Clean Technology Index  
710 JB: The Jarque-Bera test  
711 Q20: Ljung-Box statistics 20  
712 ARCH-LM: Autoregressive Conditional Heteroskedasticity-Lagrange Multiplier tests  
713 ADF: Augmented Dickey and Fuller  
714 PP: Phillips and Perron  
715 KPSS: Kwiatkowski et al. (1992) stationarity test  
716 Corr.: Pearson correlation  
717 CWT: Continuous wavelet transform  
718 DWT: Discrete wavelet transform  
719 VAR: vector autoregressive  
720 AIC: The Akaike information criterion

721 **Acknowledgments:** Supports from the “Double-First Class” Think Tank Program of  
722 China University of Mining and Technology (No.2018WHCC01) are acknowledged.

723 **Authors’ contributions:** Data curation, N.L.; Formal analysis, N.L.; Funding  
724 acquisition, N.L. and C.L.; Investigation, N.L. and C.L.; Methodology, N.L.; Resources,  
725 N.L. and C.L.; Software, N.L.; Supervision, C.L.; Validation, N.L.; Visualization, N.L.;  
726 Writing—original draft, N.L.; Writing—review & editing, C.L.

727 **Funding:** This research was funded by “Double-First Class” Think Tank Program of China  
728 University of Mining and Technology (No.2018WHCC01).

#### 729 **Availability of data and materials**

730 The datasets obtained and analyzed in the current study are available from the  
731 corresponding author on reasonable request.

#### 732 **Ethics approval and consent to participate**

733 Not applicable.

#### 734 **Consent for publication**

735 All authors agreed to publish the paper.

736 **Competing interests**

737 The authors declare that they have no competing interests.

738 **Author details**

739 <sup>1</sup> School of Management, China University of Mining & Technology, Xuzhou 221116,  
740 China.

741

742

743 **Reference**

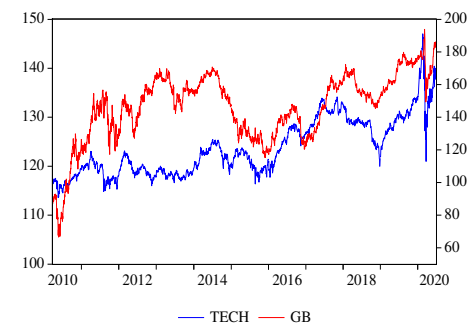
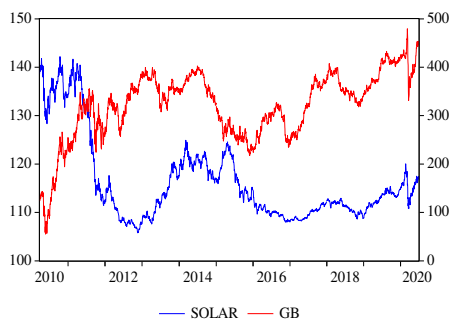
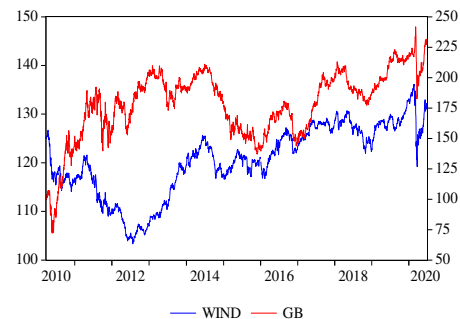
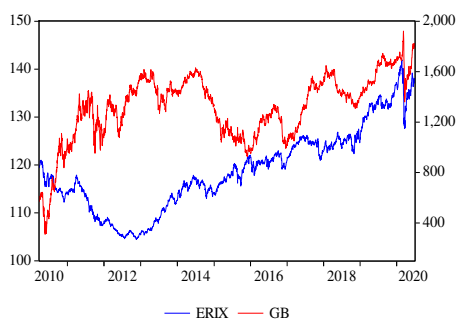
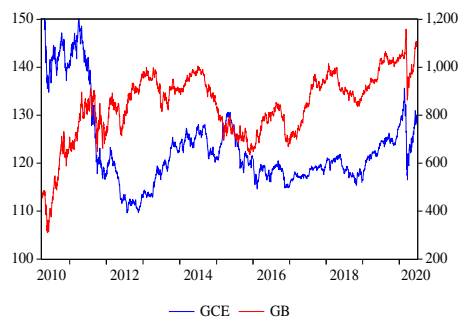
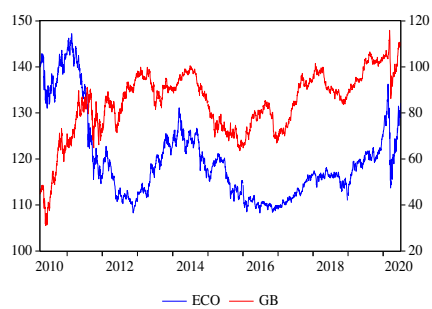
- 744 1. Le Quéré, C. ; Jackson, R. B. ; Jones, M. W. ; Smith, A. J. ; Abernethy, S. ; Andrew,  
745 R. M. ; De-Gol, A. J. ; Willis, D. R. ; Shan, Y. ; Canadell, J. G., Temporary  
746 reduction in daily global CO<sub>2</sub> emissions during the COVID-19 forced confinement.  
747 *Nature Climate Change* **2020**, 1-7.
- 748 2. McCollum, D. L. ; Echeverri, L. G. ; Busch, S. ; Pachauri, S. ; Parkinson, S. ; Rogelj,  
749 J. ; Krey, V. ; Minx, J. C. ; Nilsson, M. ; Stevance, A.-S., Connecting the  
750 sustainable development goals by their energy inter-linkages. *Environmental*  
751 *Research Letters* **2018**, 13, (3), 033006.
- 752 3. Xie, F. ; Liu, Y. ; Guan, F. ; Wang, N., How to coordinate the relationship between  
753 renewable energy consumption and green economic development: from the perspective  
754 of technological advancement. *Environmental Sciences Europe* **2020**, 32, (1), 1-15.
- 755 4. Brack, W. ; Ait-Aissa, S. ; Backhaus, T. ; Birk, S. ; Barceló, D. ; Burgess, R. ;  
756 Cousins, I. ; Dulio, V. ; Escher, B. I. ; Focks, A., Strengthen the European  
757 collaborative environmental research to meet European policy goals for achieving  
758 a sustainable, non-toxic environment. *Environmental Sciences Europe* **2019**, 31,  
759 (1), 1-9.
- 760 5. Ng, T. H. ; Tao, J. Y., Bond financing for renewable energy in Asia. *Energy Policy*  
761 **2016**, 95, 509-517.
- 762 6. Shishlov, I. ; Morel, R. ; Cochran, I., Beyond transparency: unlocking the full  
763 potential of green bonds. *Institute for Climate Economics* **2016**, 1-28.
- 764 7. Park, S. K., Investors as regulators: Green bonds and the governance challenges  
765 of the sustainable finance revolution. *Stan. J. Int'l L.* **2018**, 54, 1.
- 766 8. Azhgaliyeva, D. ; Kapoor, A. ; Liu, Y., Green bonds for financing renewable energy  
767 and energy efficiency in South-East Asia: a review of policies. *Journal of*  
768 *Sustainable Finance & Investment* **2020**, 10, (2), 113-140.
- 769 9. Hachenberg, B. ; Schiereck, D., Are green bonds priced differently from  
770 conventional bonds? *Journal of Asset Management* **2018**, 19, (6), 371-383.
- 771 10. Racheilo, V. THE GREEN BOND MARKET IN EMERGING MARKET ECONOMIES Green Bond Market  
772 Development and Green Premium analysis in Emerging Market Economies. Università  
773 Ca' Foscari Venezia, 2019.
- 774 11. Tang, D. Y. ; Zhang, Y., Do shareholders benefit from green bonds? *Journal of*  
775 *Corporate Finance* **2020**, 61, 101427.
- 776 12. Naccache, T., Oil price cycles and wavelets. *Energy Economics* **2011**, 33, (2),  
777 338-352.
- 778 13. Vacha, L. ; Barunik, J., Co-movement of energy commodities revisited: Evidence  
779 from wavelet coherence analysis. *Energy Economics* **2012**, 34, (1), 241-247.
- 780 14. Jammazi, R., Cross dynamics of oil-stock interactions: A redundant wavelet  
781 analysis. *Energy* **2012**, 44, (1), 750-777.

- 782 15. Reboredo, J. C.; Rivera-Castro, M. A., Wavelet-based evidence of the impact of  
783 oil prices on stock returns. *International Review of Economics & Finance* **2014**,  
784 29, 145-176.
- 785 16. Reboredo, J. C.; Rivera-Castro, M. A., A wavelet decomposition approach to crude  
786 oil price and exchange rate dependence. *Economic Modelling* **2013**, 32, 42-57.
- 787 17. Madaleno, M.; Pinho, C., Wavelet dynamics for oil-stock world interactions.  
788 *Energy Economics* **2014**, 45, 120-133.
- 789 18. Shiller, R. J.; Beltratti, A. E., Stock prices and bond yields: Can their  
790 comovements be explained in terms of present value models? *Journal of monetary*  
791 *economics* **1992**, 30, (1), 25-46.
- 792 19. Arouri, M. E. H.; Jouini, J.; Nguyen, D. K., Volatility spillovers between oil  
793 prices and stock sector returns: Implications for portfolio management. *Journal*  
794 *of International money and finance* **2011**, 30, (7), 1387-1405.
- 795 20. Bae, K.-H.; Karolyi, G. A.; Stulz, R. M., A new approach to measuring financial  
796 contagion. *The Review of Financial Studies* **2003**, 16, (3), 717-763.
- 797 21. Barsky, R. B. *Why don't the prices of stocks and bonds move together?*; 0898-2937;  
798 National Bureau of Economic Research: 1986.
- 799 22. Dean, C. R.; Young, A. F.; Meric, I.; Lee, C.; Wang, L.; Sorgenfrei, S.; Watanabe,  
800 K.; Taniguchi, T.; Kim, P.; Shepard, K. L., Boron nitride substrates for high-  
801 quality graphene electronics. *Nature nanotechnology* **2010**, 5, (10), 722-726.
- 802 23. Pham, L., Is it risky to go green? A volatility analysis of the green bond market.  
803 *Journal of Sustainable Finance & Investment* **2016**, 6, (4), 263-291.
- 804 24. Bachelet, M. J.; Becchetti, L.; Manfredonia, S., The green bonds premium puzzle:  
805 The role of issuer characteristics and third-party verification. *Sustainability*  
806 **2019**, 11, (4), 1098.
- 807 25. Reboredo, J. C., Green bond and financial markets: Co-movement, diversification  
808 and price spillover effects. *Energy Economics* **2018**, 74, 38-50.
- 809 26. Reboredo, J. C.; Ugolini, A., Price connectedness between green bond and  
810 financial markets. *Economic Modelling* **2019**.
- 811 27. Reboredo, J. C.; Ugolini, A.; Aiube, F. A. L., Network connectedness of green  
812 bonds and asset classes. *Energy Economics* **2020**, 86, 104629.
- 813 28. Jin, J.; Han, L.; Wu, L.; Zeng, H., The hedging effect of green bonds on carbon  
814 market risk. *International Review of Financial Analysis* **2020**, 101509.
- 815 29. Nanji, A.; Calder, A.; Kolodzie, M., Green Bonds: Fifty Shades of Green. *RBC*  
816 *Capital Markets*. Available at: [http://www.rbc.com/community-](http://www.rbc.com/community-sustainability/_assets-custom/pdf/Green-Bonds-Fifty-Shades-of-Green.pdf)  
817 *sustainability/\_assets-custom/pdf/Green-Bonds-Fifty-Shades-of-Green.pdf* **2014**.
- 818 30. Tolliver, C.; Keeley, A. R.; Managi, S., Policy targets behind green bonds for  
819 renewable energy: Do climate commitments matter? *Technological Forecasting and*  
820 *Social Change* **2020**, 157, 120051.
- 821 31. Tao, J. Y., Utilising Green Bonds for Financing Renewable Energy Projects in  
822 Developing Asian Countries. *Chapters* **2016**.
- 823 32. Liu, N.; Liu, C.; Da, B.; Zhang, T.; Guan, F., Dependence and risk spillovers  
824 between green bonds and clean energy markets. *Journal of Cleaner Production* **2020**,  
825 279, 123595.
- 826 33. Hammoudeh, S.; Ajmi, A. N.; Mokni, K., Relationship between green bonds and  
827 financial and environmental variables: A novel time-varying causality. *Energy*  
828 *Economics* **2020**, 92, 104941.
- 829 34. Nguyen, T. T. H.; Naeem, M. A.; Balli, F.; Balli, H. O.; Vo, X. V., Time-frequency  
830 comovement among green bonds, stocks, commodities, clean energy, and conventional

- 831 bonds. *Finance Research Letters* **2020**, 101739.
- 832 35. Le, T.-L.; Abakah, E. J. A.; Tiwari, A. K., Time and frequency domain  
833 connectedness and spill-over among fintech, green bonds and cryptocurrencies in  
834 the age of the fourth industrial revolution. *Technological Forecasting and Social  
835 Change* **2020**, 162, 120382.
- 836 36. Reboredo, J. C., Green bond and financial markets: Co-movement, diversification  
837 and price spillover effects. *Energy Economics* **2018**, 74, (AUG.), 38-50.
- 838 37. Ugolini; Andrea; Reboredo; Juan; C.; Rivera-Castro; Miguel; A., Wavelet-based  
839 test of co-movement and causality between oil and renewable energy stock prices.  
840 *Energy Economics* **2017**.
- 841 38. Rezec, M.; Scholtens, B., Financing energy transformation: The role of renewable  
842 energy equity indices. *International Journal of Green Energy* **2017**, 14, (4), 368-  
843 378.
- 844 39. Ahmad, W., On the dynamic dependence and investment performance of crude oil and  
845 clean energy stocks. *Research in International Business and Finance* **2017**, 42,  
846 376-389.
- 847 40. Bondia, R.; Ghosh, S.; Kanjilal, K., International crude oil prices and the stock  
848 prices of clean energy and technology companies: evidence from non-linear  
849 cointegration tests with unknown structural breaks. *Energy* **2016**, 101, 558-565.
- 850 41. Reboredo, J. C., Is there dependence and systemic risk between oil and renewable  
851 energy stock prices? *Energy Economics* **2015**, 48, 32-45.
- 852 42. Lundgren, A. I.; Milicevic, A.; Uddin, G. S.; Kang, S. H., Connectedness network  
853 and dependence structure mechanism in green investments. *Energy Economics* **2018**,  
854 72, 145-153.
- 855 43. Torrence, C.; Compo, G. P., A practical guide to wavelet analysis. *Bulletin of  
856 the American Meteorological society* **1998**, 79, (1), 61-78.
- 857 44. Torrence, C.; Webster, P. J., Interdecadal changes in the ENSO - monsoon system.  
858 *Journal of climate* **1999**, 12, (8), 2679-2690.
- 859 45. Berry, W.; Aggarwal, R.; Inclan, C., Detecting volatility changes across the oil  
860 sector. *The Journal of Futures Markets (1986-1998)* **1996**, 47, (1), 313.
- 861 46. Abhyankar, A., Does the stock index futures market tend to lead the cash? New  
862 evidence from the FT-SE 100 stock index futures market. In *Working Paper No. 96-  
863 01, Department of Accounting and Finance University of Stirling*, 1996.
- 864 47. Chen, A.-S.; Wuh Lin, J., Cointegration and detectable linear and nonlinear  
865 causality: analysis using the London Metal Exchange lead contract. *Applied  
866 Economics* **2004**, 36, (11), 1157-1167.
- 867 48. Bekiros, S. D.; Diks, C. G., The relationship between crude oil spot and futures  
868 prices: Cointegration, linear and nonlinear causality. *Energy Economics* **2008**,  
869 30, (5), 2673-2685.
- 870 49. Baek, E. G.; Brock, W. A., A nonparametric test for independence of a multivariate  
871 time series. *Statistica Sinica* **1992**, 137-156.
- 872 50. Hiemstra, C.; Jones, J. D., Testing for linear and nonlinear Granger causality  
873 in the stock price - volume relation. *The Journal of Finance* **1994**, 49, (5), 1639-  
874 1664.
- 875 51. Diks, C.; Panchenko, V., A new statistic and practical guidelines for  
876 nonparametric Granger causality testing. *Journal of Economic Dynamics and Control*  
877 **2006**, 30, (9-10), 1647-1669.
- 878 52. Akoum, I.; Graham, M.; Kivihaho, J.; Nikkinen, J.; Omran, M., Co-movement of oil  
879 and stock prices in the GCC region: A wavelet analysis. *The Quarterly Review of*

880  
881  
882  
883  
884  
885  
886  
887  
888  
889  
890  
891  
892  
893  
894  
895  
896  
897  
898  
899  
900  
901  
902  
903  
904  
905  
906  
907  
908  
909  
910  
911  
912  
913

*Economics and Finance* **2012**, 52, (4), 385-394.  
53. Ranta, M., Contagion among major world markets: a wavelet approach. *International Journal of Managerial Finance* **2013**.  
54. Yu, L.; Li, J.; Tang, L.; Wang, S., Linear and nonlinear Granger causality investigation between carbon market and crude oil market: A multi-scale approach. *Energy Economics* **2015**, 51, 300-311.



914

915 Fig.1. Time-series plot of the green bonds and renewable energy pairs. Note: The left axis  
916 represents the green bond index price level. The right axis represents the renewable energy  
917 price level.

918

919

920

921

922

923

924

925

926

927

928

929

930

931

932

933

934

935

936

937

938

939

940

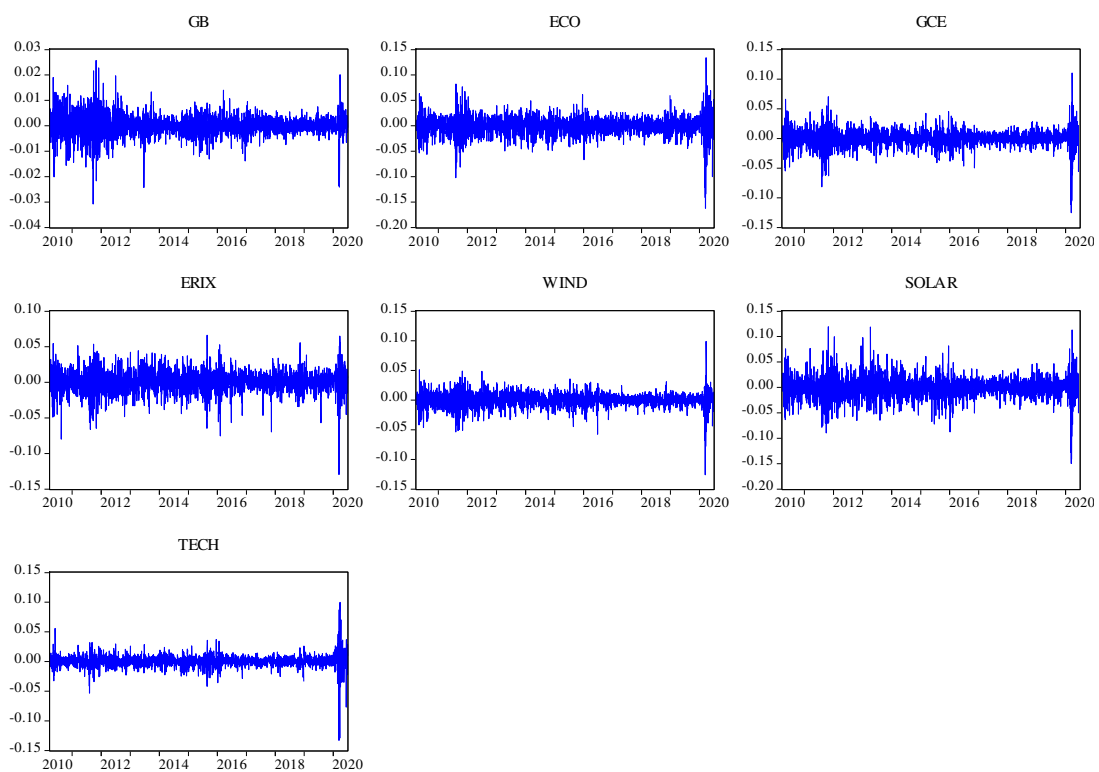
941

942

943

944

945



946

947

948

Fig. 2. Time-series plot of green bonds and renewable energy returns.

949

950

951

952

953

954

955

956

957

958

959

960

961

962

963

964

965

966

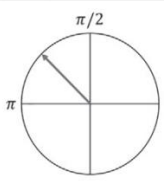
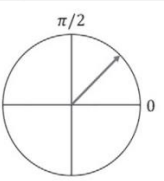
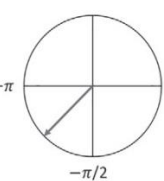
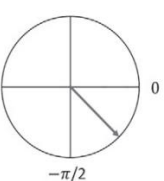
967

968

969

970

971

Out-of-Phase	In-Phase
	
<i>Y leads X</i>	<i>X leads Y</i>
	
<i>X leads Y</i>	<i>Y leads X</i>

972

973

974

975

976

977

978

979

980

981

982

Fig.3. Phase interpretation

983

984

985

986

987

988

989

990

991

992

993

994

995

996

997

998

999

1000

1001

1002

1003

1004

1005

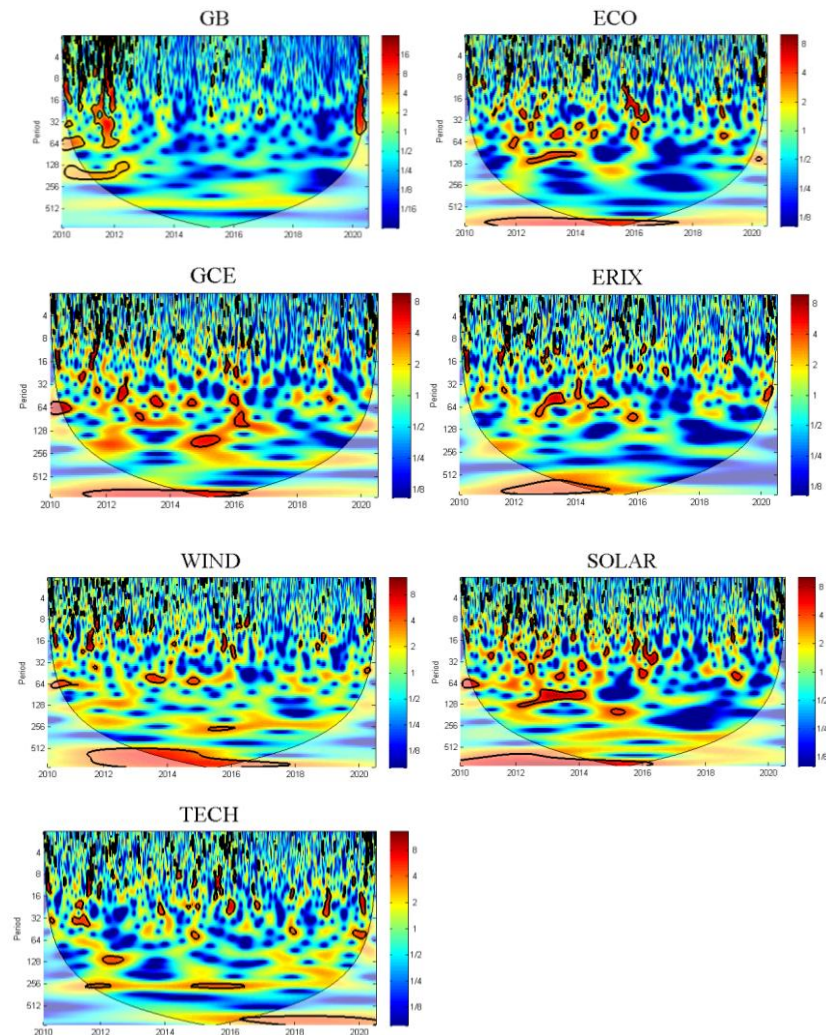
1006

1007

1008

1009

1010



1011

1012 Fig.4. Continuous wavelet transforms for the green bonds and six renewable energy  
1013 markets. Note: The dark red (blue) indicates strong (smooth) fluctuations and the bold  
1014 black outline indicates the wavelet power spectrum generated from the Monte Carlo  
1015 simulation of the 5% significance level. The region affected by the edge effect is  
1016 represented by the black curve and defines the cone of influence. The horizontal axis  
1017 indicates time (year) and the vertical axis indicates period (day).

1018

1019

1020

1021

1022

1023

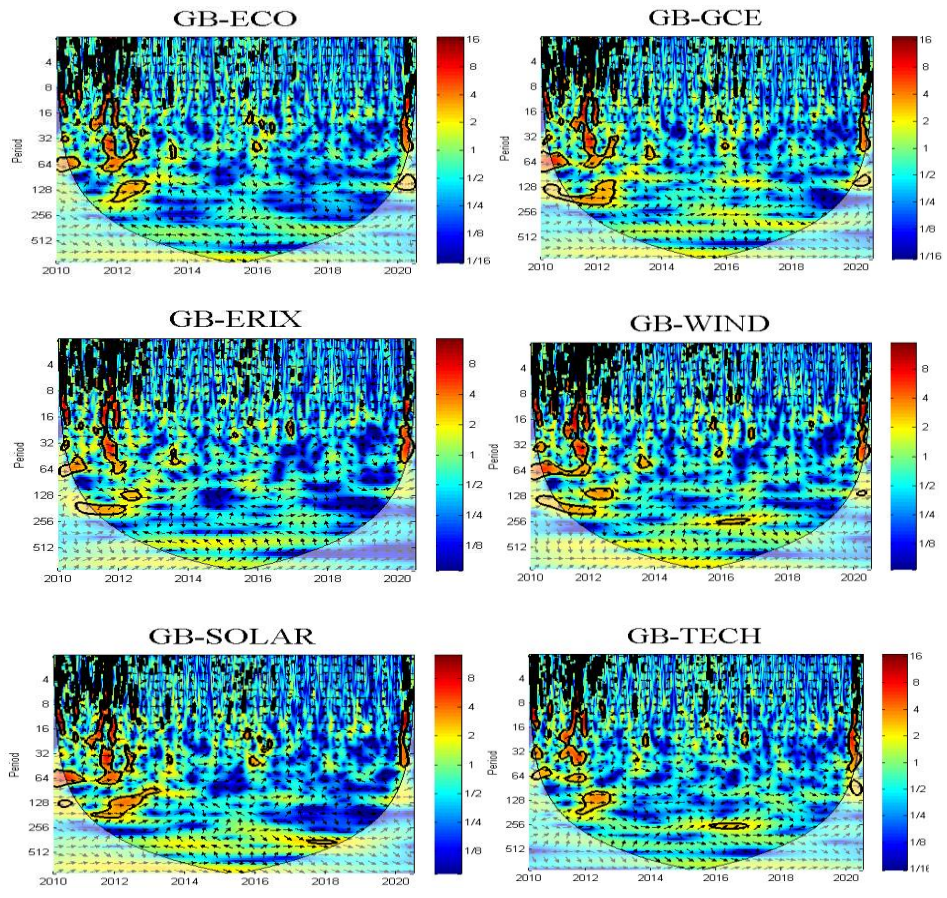
1024

1025

1026

1027

1028



1029

1030

1031

1032

1033

1034

1035

1036

1037

1038

1039

1040

1041

1042

1043

1044

1045 Fig. 5. Cross-wavelet transforms for green bonds and renewable energy indices. Note: the  
1046 horizontal axis presents time and the vertical axis shows frequency (days). The warmer  
1047 color of the region, the higher the dependence between the pairs.

1048

1049

1050

1051

1052

1053

1054

1055

1056

1057

1058

1059

1060

1061

1062

1063

1064

1065

1066

1067

1068

1069

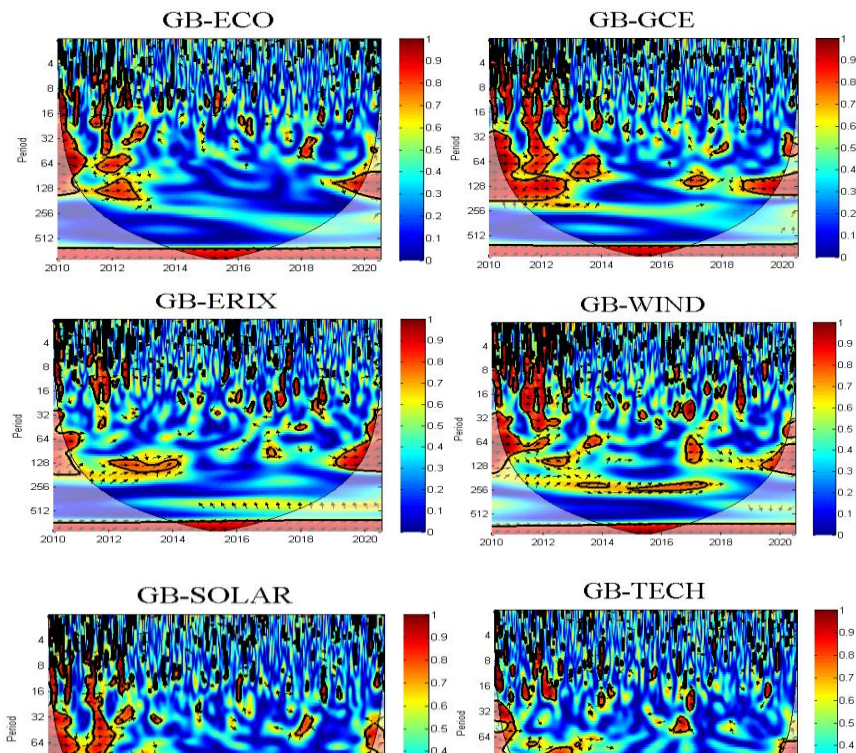
1070

1071

1072

1073

1074



1075  
 1076  
 1077  
 1078  
 1079  
 1080  
 1081  
 1082  
 1083  
 1084  
 1085  
 1086  
 1087  
 1088

Fig.6. Wavelet coherence of green bonds and renewable energy pairs. Note: refer to Fig.4.

Table1. Descriptive statistics for green bonds and renewable energy return series.

	GB	ECO	GCE	ERIX	WIND	SOLAR	TECH
Mean	0.0001	-0.0001	-0.0001	0.0002	0.0001	-0.0003	0.0002
Maximum	0.026	0.134	0.110	0.066	0.099	0.120	0.100
Minimum	-0.031	-0.162	-0.125	-0.130	-0.126	-0.150	-0.133
Std. Dev.	0.004	0.018	0.014	0.015	0.012	0.021	0.011
Skewness	-0.31	-0.75	-0.75	-0.54	-0.72	-0.19	-1.46
Kurtosis	8.43	11.23	12.29	7.19	12.37	7.30	33.99
JB	3321.7	7793.4	9843.3	2081.0	9996.7	2072.9	107807.4
ADF	-51.40	-32.96	-18.13	-49.55	-32.74	-44.30	-19.33
PP	-51.41	-51.18	-46.60	-49.54	-46.92	-44.41	-54.09
KPSS	0.11	0.30	0.32	0.43	0.22	0.30	0.04
Q (20)	30.36*	85.86***	118.58***	32.64**	76.98***	109.39***	116.08***
ARCH-LM (5)	31.17***	37.23***	48.93***	24.77***	31.99***	29.98***	29.14***
Corr.	1.00	0.22	0.37	0.26	0.50	0.26	0.15

1089 Note: Daily data between March 29, 2010 and June 30, 2020. Notes. JB is used to test for  
 1090 normality Jarque-Bera  $\chi^2$  statistic. Q (20) denotes the Ljung-Box statistics for serial returns  
 1091 computed with 20 lags. ARCH-LM (5) is Engle's heteroscedasticity LM test, calculated  
 1092 using 5 lags. ADF, PP, and KPSS stand for Augmented Dickey and Fuller (1979) and  
 1093 Phillips and Perron (1988) unit root test and Kwiatkowski et al. (1992) stationarity test,  
 1094 respectively. Corr. is the Pearson correlation for each renewable energy index with green  
 1095 bonds. As usual, \*\*\*, \*\*and \* denote significance at 1%, 5% and 10%, respectively.

1096

1097  
1098  
1099  
1100  
1101  
1102  
1103  
1104  
1105  
1106  
1107  
1108  
1109  
1110  
1111

Table 2 Linear Granger causality test on returns

Variables	Lags	H0: GB does not cause RE		H0: RE does not cause GB		Results
		F-test	P-Value	F-test	P-Value	
GB & ECO	7	1.925	0.0618	9.494	0.000	GB ← ECO
GB & GCE	10	2.571	0.004	5.762	0.000	GB ⇔ GCE
GB & ERIX	5	3.021	0.010	2.996	0.011	GB ⇔ ERIX
GB & WIND	10	2.391	0.008	3.233	0.000	GB ⇔ WIND
GB & SOLAR	7	1.803	0.083	7.086	0.000	GB ← SOLAR
GB & TECH	10	3.539	0.000	4.133	0.000	GB ⇔ TECH

1112 Note: GB refer to green bonds. RE stands for renewable energy. The lag number is  
1113 determined based on the AIC criterion.

1114 (Source: Authors' calculation.)

1115  
1116  
1117  
1118  
1119  
1120  
1121

1122  
 1123  
 1124  
 1125  
 1126  
 1127  
 1128  
 1129  
 1130  
 1131  
 1132  
 1133  
 1134  
 1135  
 1136  
 1137

Table 3 Multi-scale linear Granger causality test on returns

Variables	Lags	H0: GB does not cause RE		H0: RE does not cause GB		Results
		F-test	P-Value	F-test	P-Value	
<b>Panel A: D1</b>						
GB & ECO	10	1.158	0.315	2.369	0.009	GB ← ECO
GB & GCE	10	1.730	0.069	2.419	0.007	GB ← GCE
GB & ERIX	10	2.171	0.017	1.674	0.081	GB ⇔ ERIX
GB & WIND	10	0.935	0.499	2.002	0.030	GB ← WIND
GB & SOLAR	10	0.657	0.765	2.507	0.005	GB ← SOLAR
GB & TECH	10	1.515	0.128	1.072	0.381	No causality
<b>Panel B: D2</b>						
GB & ECO	10	3.468	0.000	3.015	0.001	GB ⇔ ECO
GB & GCE	10	2.078	0.023	2.050	0.025	GB ⇔ GCE
GB & ERIX	10	1.008	0.434	1.596	0.101	No causality
GB & WIND	10	2.034	0.027	1.854	0.047	GB ⇔ WIND
GB & SOLAR	10	1.955	0.034	1.330	0.208	GB → SOLAR
GB & TECH	10	4.104	0.000	4.050	0.000	GB ⇔ TECH
<b>Panel C: D3</b>						
GB & ECO	10	5.669	0.000	6.263	0.000	GB ⇔ ECO
GB & GCE	10	7.379	0.000	6.717	0.000	GB ⇔ GCE
GB & ERIX	10	6.399	0.000	7.038	0.000	GB ⇔ ERIX

GB & WIND	10	7.091	0.000	6.726	0.000	GB $\Leftrightarrow$ WIND
GB & SOLAR	10	4.387	0.000	4.570	0.000	GB $\Leftrightarrow$ SOLAR
GB & TECH	10	5.105	0.000	4.926	0.000	GB $\Leftrightarrow$ TECH
<b>Panel D: D4</b>						
GB & ECO	10	5.717	0.000	3.653	0.000	GB $\Leftrightarrow$ ECO
GB & GCE	10	3.804	0.000	2.805	0.002	GB $\Leftrightarrow$ GCE
GB & ERIX	10	5.135	0.000	2.732	0.002	GB $\Leftrightarrow$ ERIX
GB & WIND	10	4.368	0.000	1.395	0.176	GB $\rightarrow$ WIND
GB & SOLAR	10	3.894	0.000	3.066	0.001	GB $\Leftrightarrow$ SOLAR
GB & TECH	10	2.840	0.002	3.113	0.001	GB $\Leftrightarrow$ TECH
<b>Panel E: D5</b>						
GB & ECO	10	0.323	0.975	0.816	0.613	No causality
GB & GCE	10	1.156	0.316	5.164	0.000	GB $\leftarrow$ GCE
GB & ERIX	10	2.839	0.002	3.041	0.001	GB $\Leftrightarrow$ ERIX
GB & WIND	10	2.477	0.006	3.590	0.000	GB $\Leftrightarrow$ WIND
GB & SOLAR	10	0.634	0.786	1.787	0.058	No causality
GB & TECH	10	0.678	0.746	0.467	0.912	No causality
<b>Panel F: D6</b>						
GB & ECO	10	2.694	0.003	0.807	0.622	GB $\rightarrow$ ECO
GB & GCE	10	4.253	0.000	0.448	0.923	GB $\rightarrow$ GCE
GB & ERIX	10	5.309	0.000	0.296	0.982	GB $\rightarrow$ ERIX
GB & WIND	10	2.847	0.002	0.463	0.914	GB $\rightarrow$ WIND
GB & SOLAR	10	5.671	0.000	0.578	0.833	GB $\rightarrow$ SOLAR
GB & TECH	10	2.328	0.010	1.288	0.231	GB $\rightarrow$ TECH
<b>Panel G: D7</b>						
GB & ECO	10	0.124	1.000	-0.279	1.000	No causality
GB & GCE	10	-0.128	1.000	0.216	0.995	No causality
GB & ERIX	10	14.372	0.000	12.175	0.000	GB $\Leftrightarrow$ ERIX
GB & WIND	10	4.086	0.000	2.673	0.003	GB $\Leftrightarrow$ WIND
GB & SOLAR	10	0.825	0.605	1.625	0.093	No causality
GB & TECH	10	1.614	0.096	1.805	0.055	No causality
<b>Panel H: D8</b>						
GB & ECO	3	11.815	0.000	5.804	0.001	GB $\Leftrightarrow$ ECO
GB & GCE	3	9.978	0.000	12.695	0.000	GB $\Leftrightarrow$ GCE
GB & ERIX	3	9.094	0.000	10.126	0.000	GB $\Leftrightarrow$ ERIX
GB & WIND	3	14.630	0.000	22.698	0.000	GB $\Leftrightarrow$ WIND
GB & SOLAR	3	3.075	0.027	14.145	0.000	GB $\Leftrightarrow$ SOLAR
GB & TECH	3	113.929	0.000	24.713	0.000	GB $\Leftrightarrow$ TECH

1138 Note:(refer to table 2.)

1139

1140

1141

1142

1143  
 1144  
 1145  
 1146  
 1147  
 1148  
 1149  
 1150  
 1151  
 1152  
 1153  
 1154  
 1155  
 1156  
 1157  
 1158  
 1159  
 1160  
 1161  
 1162  
 1163  
 1164

Table 4 Non-linear Granger causality test on returns

Variables	H0: GB does not cause RE		H0: RE does not cause GB		Results
	T-test	P-Value	T-test	P-Value	
GB & ECO	3.333	0.000	4.069	0.000	GB $\Leftrightarrow$ ECO
GB & GCE	4.970	0.000	4.438	0.000	GB $\Leftrightarrow$ GCE
GB & ERIX	3.265	0.001	2.588	0.005	GB $\Leftrightarrow$ ERIX
GB & WIND	4.830	0.000	3.994	0.000	GB $\Leftrightarrow$ WIND
GB & SOLAR	4.472	0.000	4.301	0.000	GB $\Leftrightarrow$ SOLAR
GB & TECH	2.818	0.002	2.541	0.006	GB $\Leftrightarrow$ TECH

1165  
 1166  
 1167  
 1168

Note:(refer to table 2.)

1169  
 1170  
 1171  
 1172  
 1173  
 1174  
 1175  
 1176  
 1177  
 1178  
 1179  
 1180  
 1181  
 1182  
 1183  
 1184  
 1185  
 1186  
 1187  
 1188  
 1189  
 1190  
 1191  
 1192

Table 5 Multi-scale non-linear Granger causality test on returns

Time scale	H0: GB does not cause		H0: RE does not cause		Results
	RE		GB		
	T-test	P-Value	T-test	P-Value	
<b>Panel A: D1</b>					
GB & ECO	3.059	0.001	3.627	0.000	GB $\Leftrightarrow$ ECO
GB & GCE	4.634	0.000	4.386	0.000	GB $\Leftrightarrow$ GCE
GB & ERIX	2.514	0.006	2.179	0.015	GB $\Leftrightarrow$ ERIX
GB & WIND	4.521	0.000	5.039	0.000	GB $\Leftrightarrow$ WIND
GB & SOLAR	4.246	0.000	4.218	0.000	GB $\Leftrightarrow$ SOLAR
GB & TECH	2.145	0.016	2.716	0.003	GB $\Leftrightarrow$ TECH
<b>Panel B: D2</b>					

GB & ECO	2.785	0.003	2.052	0.020	GB $\Leftrightarrow$ ECO
GB & GCE	4.847	0.000	3.282	0.001	GB $\Leftrightarrow$ GCE
GB & ERIX	3.716	0.000	2.104	0.018	GB $\Leftrightarrow$ ERIX
GB & WIND	5.538	0.000	3.950	0.000	GB $\Leftrightarrow$ WIND
GB & SOLAR	3.615	0.000	2.641	0.004	GB $\Leftrightarrow$ SOLAR
GB & TECH	2.039	0.021	2.151	0.016	GB $\Leftrightarrow$ TECH
<b>Panel C: D3</b>					
GB & ECO	5.046	0.000	3.315	0.000	GB $\Leftrightarrow$ ECO
GB & GCE	6.579	0.000	6.278	0.000	GB $\Leftrightarrow$ GCE
GB & ERIX	5.553	0.000	4.814	0.000	GB $\Leftrightarrow$ ERIX
GB & WIND	6.000	0.000	6.945	0.000	GB $\Leftrightarrow$ WIND
GB & SOLAR	4.451	0.000	3.466	0.000	GB $\Leftrightarrow$ SOLAR
GB & TECH	4.072	0.000	3.061	0.001	GB $\Leftrightarrow$ TECH
<b>Panel D: D4</b>					
GB & ECO	3.366	0.000	1.711	0.044	GB $\Leftrightarrow$ ECO
GB & GCE	4.173	0.000	3.521	0.000	GB $\Leftrightarrow$ GCE
GB & ERIX	2.600	0.005	1.104	0.135	GB $\rightarrow$ ERIX
GB & WIND	3.911	0.000	3.245	0.001	GB $\Leftrightarrow$ WIND
GB & SOLAR	2.996	0.001	0.796	0.213	GB $\rightarrow$ SOLAR
GB & TECH	2.929	0.002	2.442	0.007	GB $\Leftrightarrow$ TECH
<b>Panel E: D5</b>					
GB & ECO	2.411	0.008	2.387	0.009	GB $\Leftrightarrow$ ECO
GB & GCE	3.180	0.001	2.508	0.006	GB $\Leftrightarrow$ GCE
GB & ERIX	2.292	0.011	1.668	0.048	GB $\Leftrightarrow$ ERIX
GB & WIND	3.689	0.000	2.216	0.013	GB $\Leftrightarrow$ WIND
GB & SOLAR	2.567	0.005	2.241	0.013	GB $\Leftrightarrow$ SOLAR
GB & TECH	0.583	0.280	2.497	0.006	GB $\leftarrow$ TECH
<b>Panel F: D6</b>					
GB & ECO	3.510	0.000	1.709	0.044	GB $\Leftrightarrow$ ECO
GB & GCE	4.016	0.000	3.725	0.000	GB $\Leftrightarrow$ GCE
GB & ERIX	2.935	0.002	2.173	0.015	GB $\Leftrightarrow$ ERIX
GB & WIND	4.474	0.000	4.062	0.000	GB $\Leftrightarrow$ WIND
GB & SOLAR	3.680	0.000	3.083	0.001	GB $\Leftrightarrow$ SOLAR
GB & TECH	2.550	0.005	2.569	0.005	GB $\Leftrightarrow$ TECH
<b>Panel G: D7</b>					
GB & ECO	-2.456	0.993	-2.661	0.996	No causality
GB & GCE	1.987	0.023	2.969	0.001	GB $\Leftrightarrow$ GCE
GB & ERIX	-3.423	1.000	3.413	0.000	GB $\leftarrow$ ERIX
GB & WIND	1.652	0.049	3.568	0.000	GB $\Leftrightarrow$ WIND
GB & SOLAR	0.070	0.472	0.761	0.223	No causality
GB & TECH	-3.249	0.999	-1.352	0.912	No causality
<b>Panel H: D8</b>					
GB & ECO	-0.338	0.632	2.226	0.013	GB $\leftarrow$ ECO
GB & GCE	1.860	0.031	0.413	0.340	GB $\rightarrow$ GCE

GB & ERIX	0.618	0.268	-2.373	0.991	No causality
GB & WIND	2.126	0.017	-2.603	0.995	GB → WIND
GB & SOLAR	1.587	0.056	0.988	0.162	No causality
GB & TECH	2.473	0.007	4.242	0.000	GB ⇔ TECH

1193 Note:(refer to table 2.)

# Figures

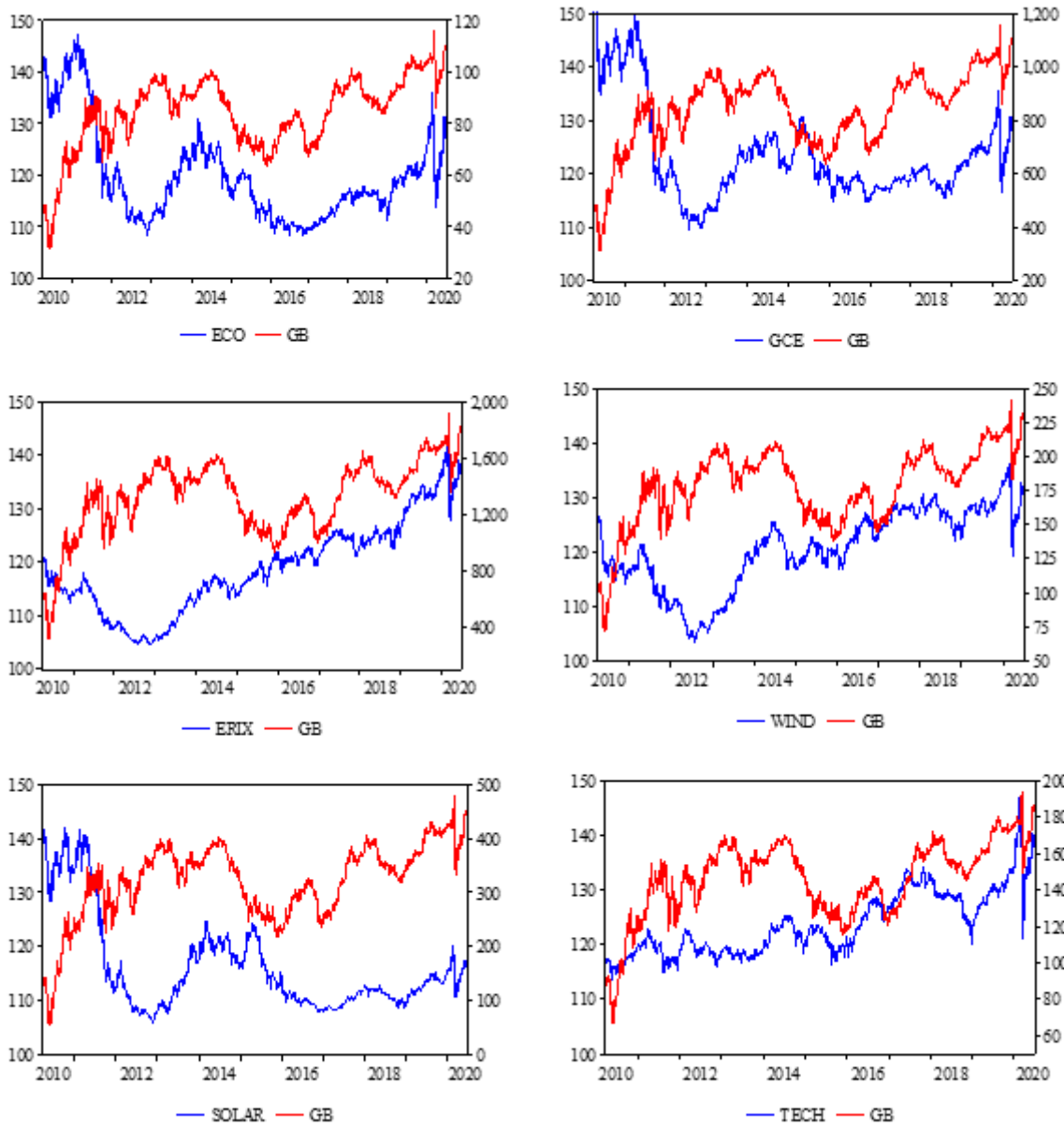
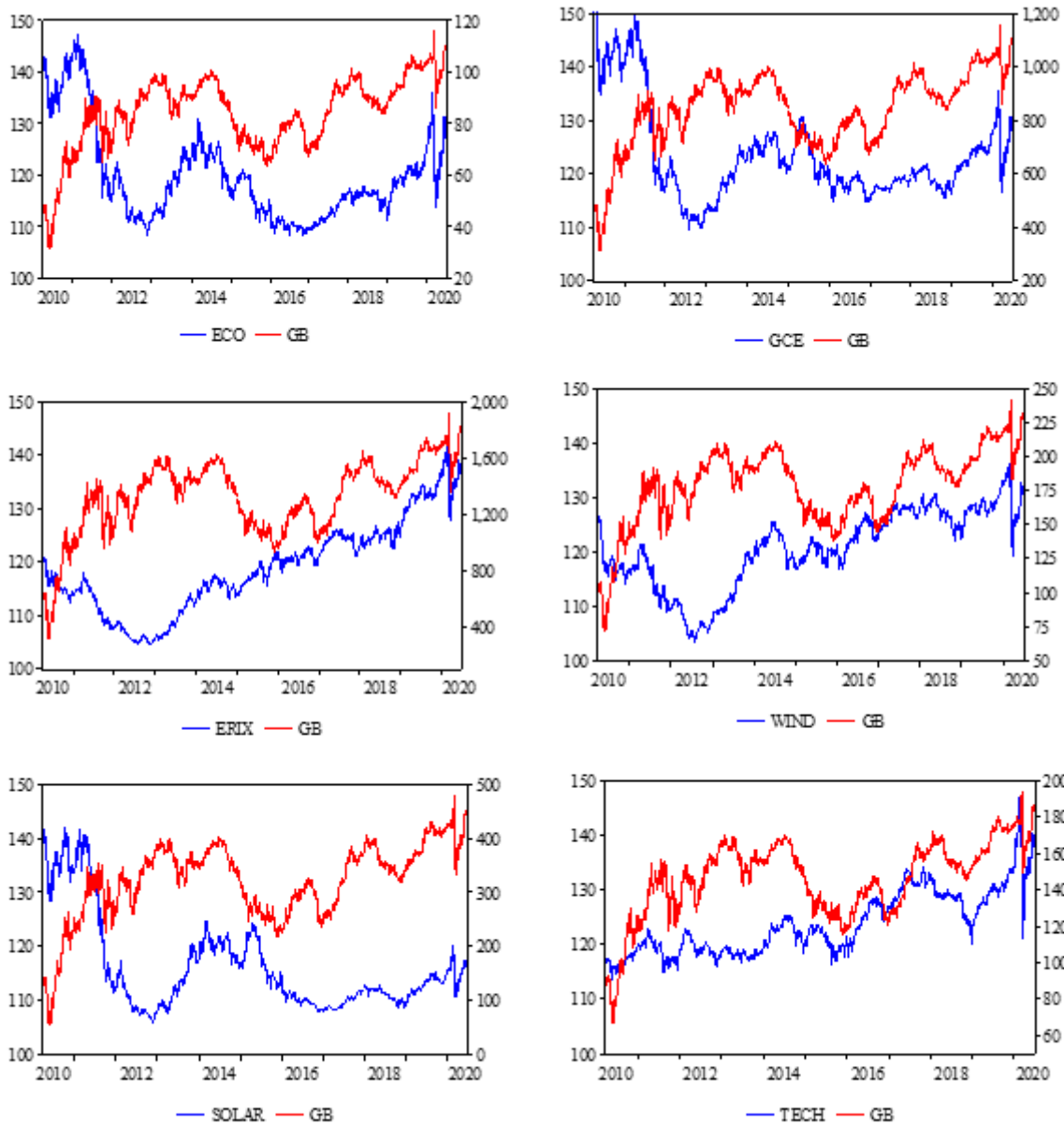


Figure 1

Time-series plot of the green bonds and renewable energy pairs. Note: The left axis represents the green bond index price level. The right axis represents the renewable energy price level.



**Figure 1**

Time-series plot of the green bonds and renewable energy pairs. Note: The left axis represents the green bond index price level. The right axis represents the renewable energy price level.

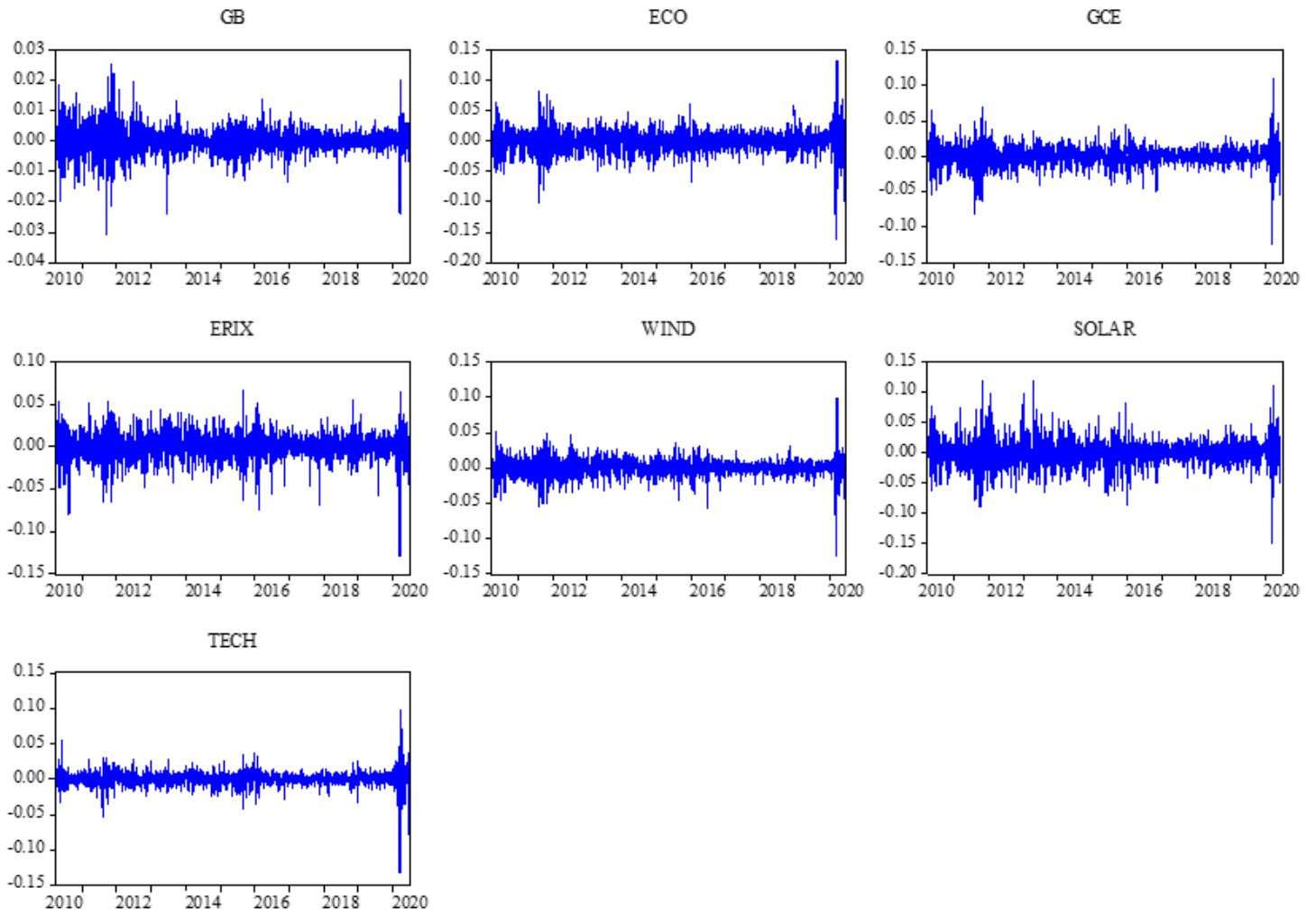


**Figure 2**

Time-series plot of green bonds and renewable energy returns.

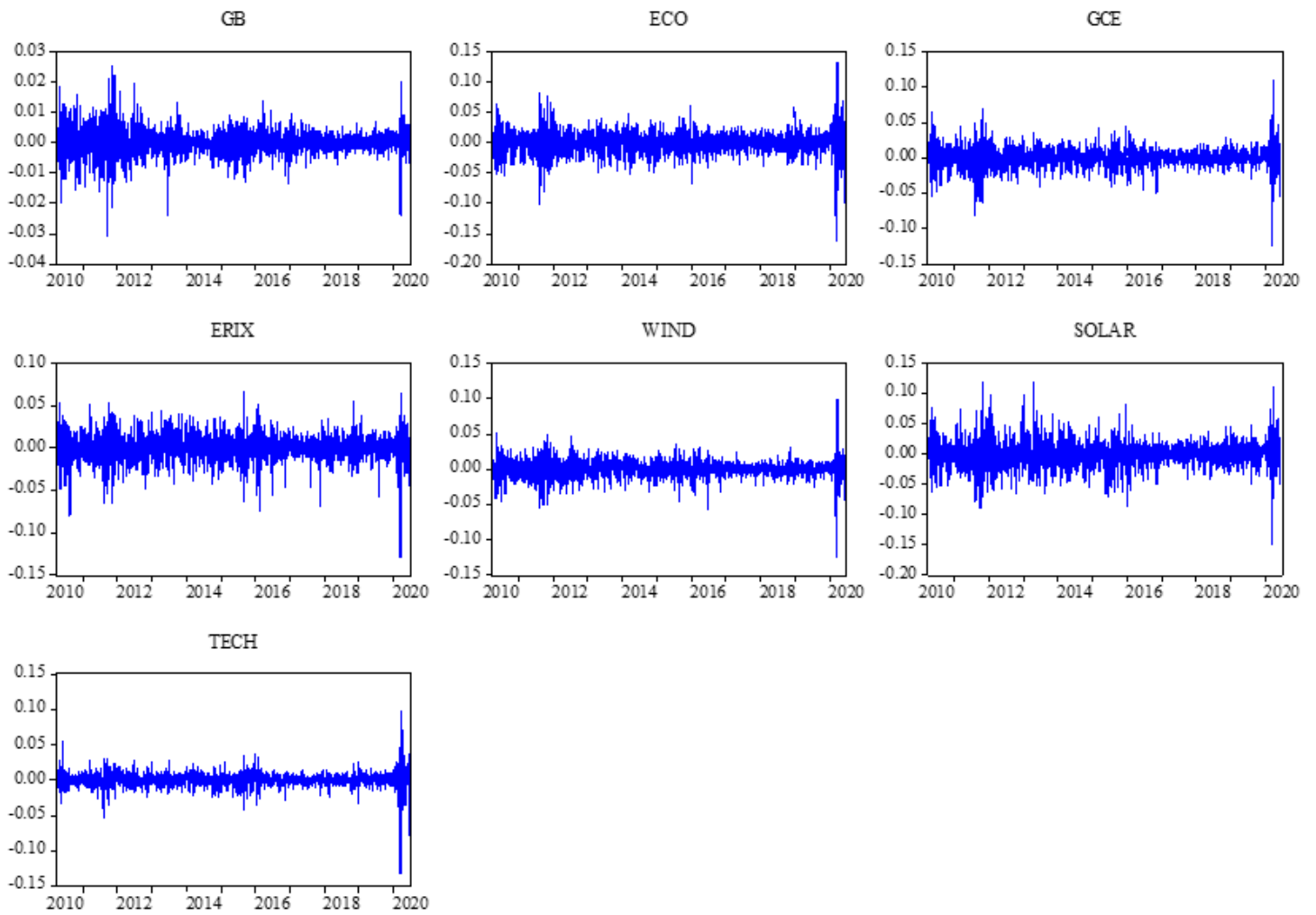


**Figure 2**

Time-series plot of green bonds and renewable energy returns.

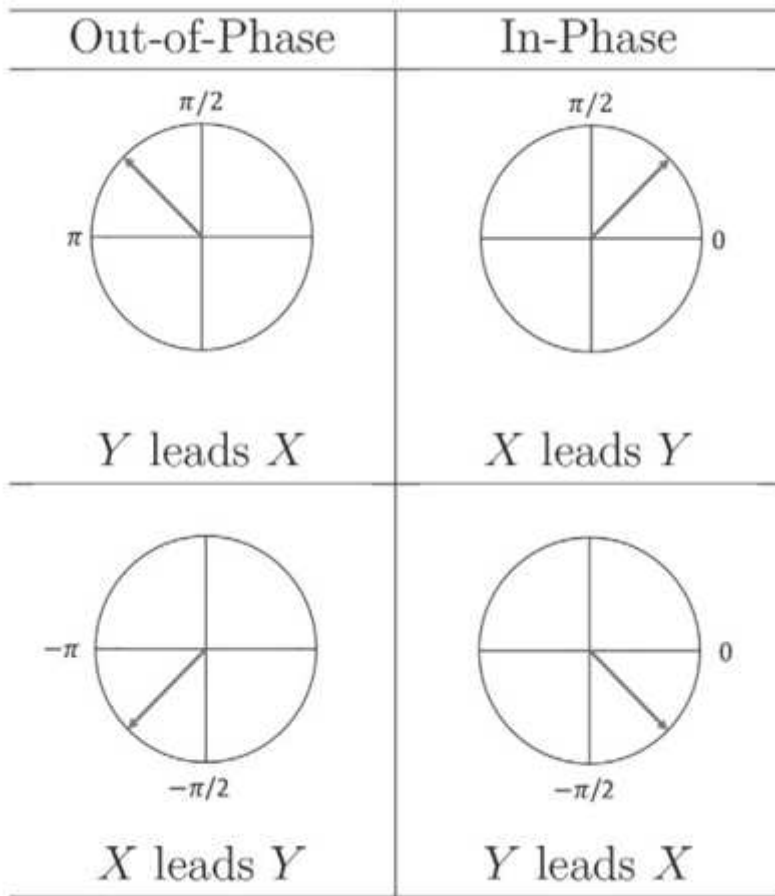


**Figure 3**

Phase interpretation

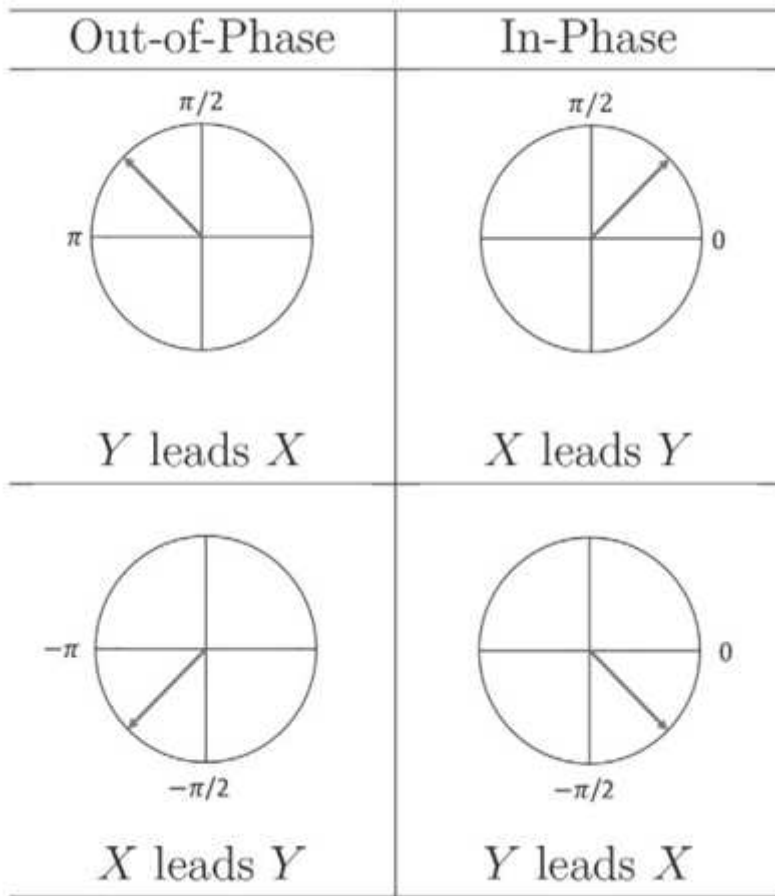


**Figure 3**

Phase interpretation

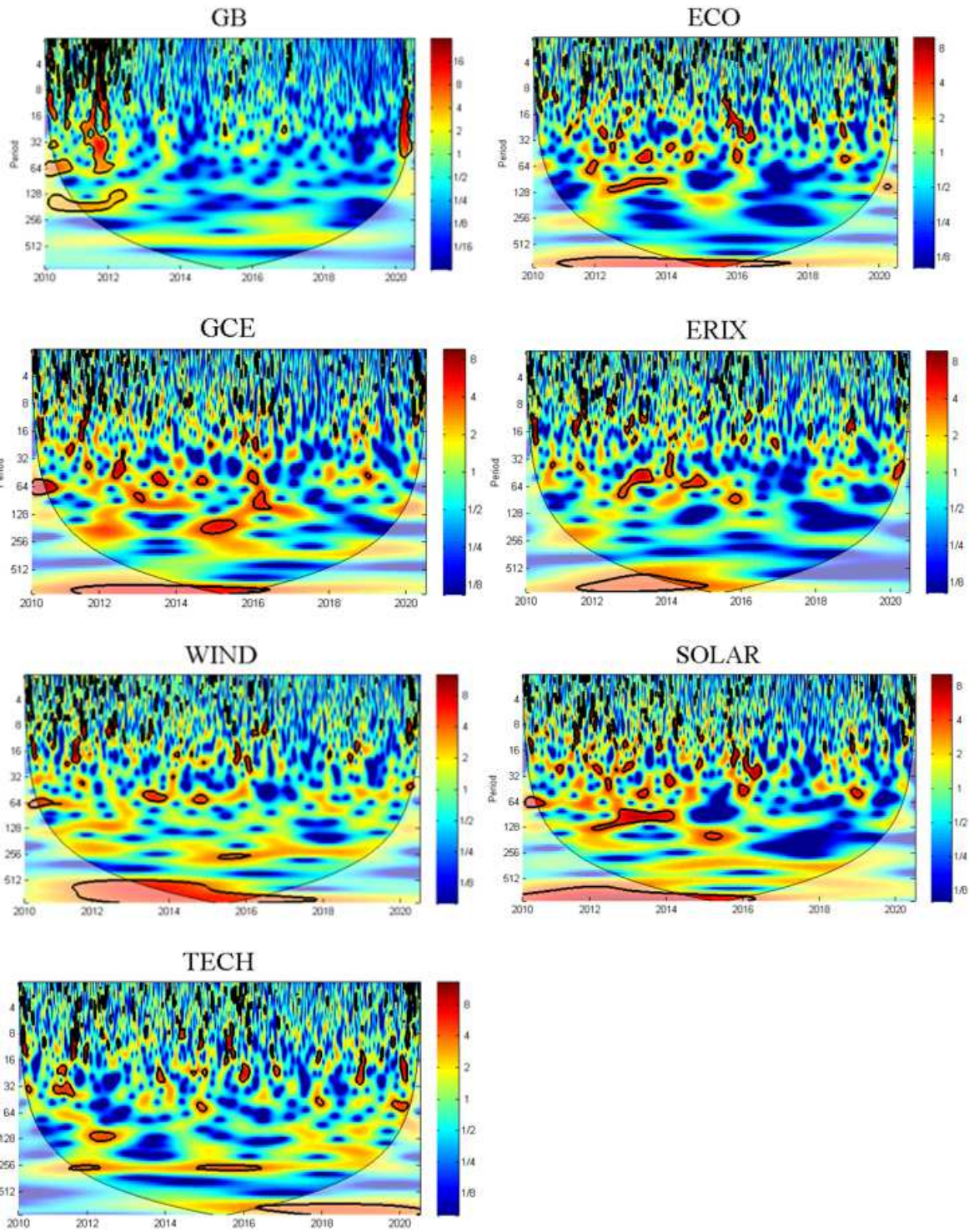


**Figure 4**

Continuous wavelet transforms for the green bonds and six renewable energy markets. Note: The dark red (blue) indicates strong (smooth) fluctuations and the bold black outline indicates the wavelet power spectrum generated from the Monte Carlo simulation of the 5% significance level. The region affected by the edge effect is represented by the black curve and defines the cone of influence. The horizontal axis indicates time (year) and the vertical axis indicates period (day).

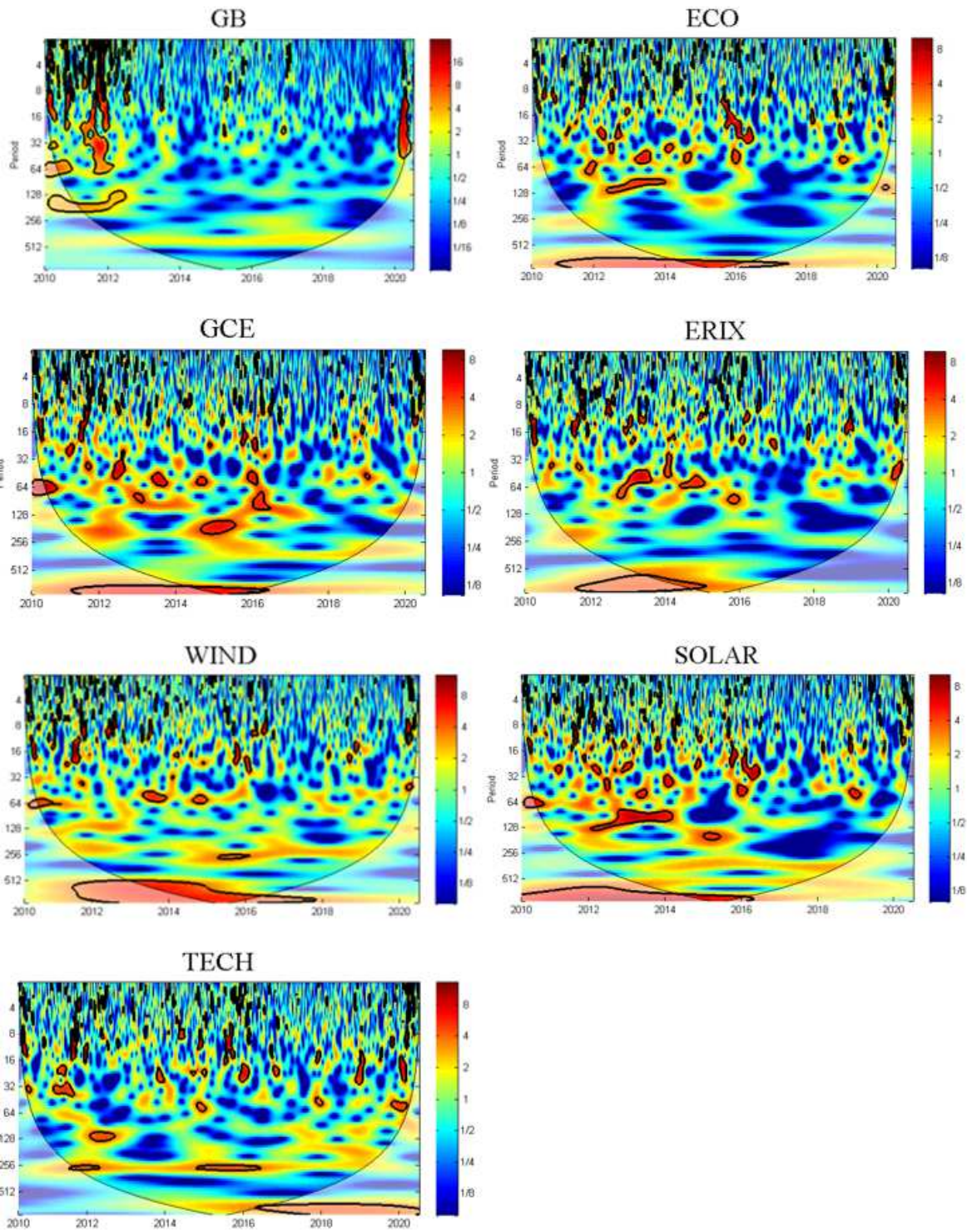


**Figure 4**

Continuous wavelet transforms for the green bonds and six renewable energy markets. Note: The dark red (blue) indicates strong (smooth) fluctuations and the bold black outline indicates the wavelet power spectrum generated from the Monte Carlo simulation of the 5% significance level. The region affected by the edge effect is represented by the black curve and defines the cone of influence. The horizontal axis indicates time (year) and the vertical axis indicates period (day).

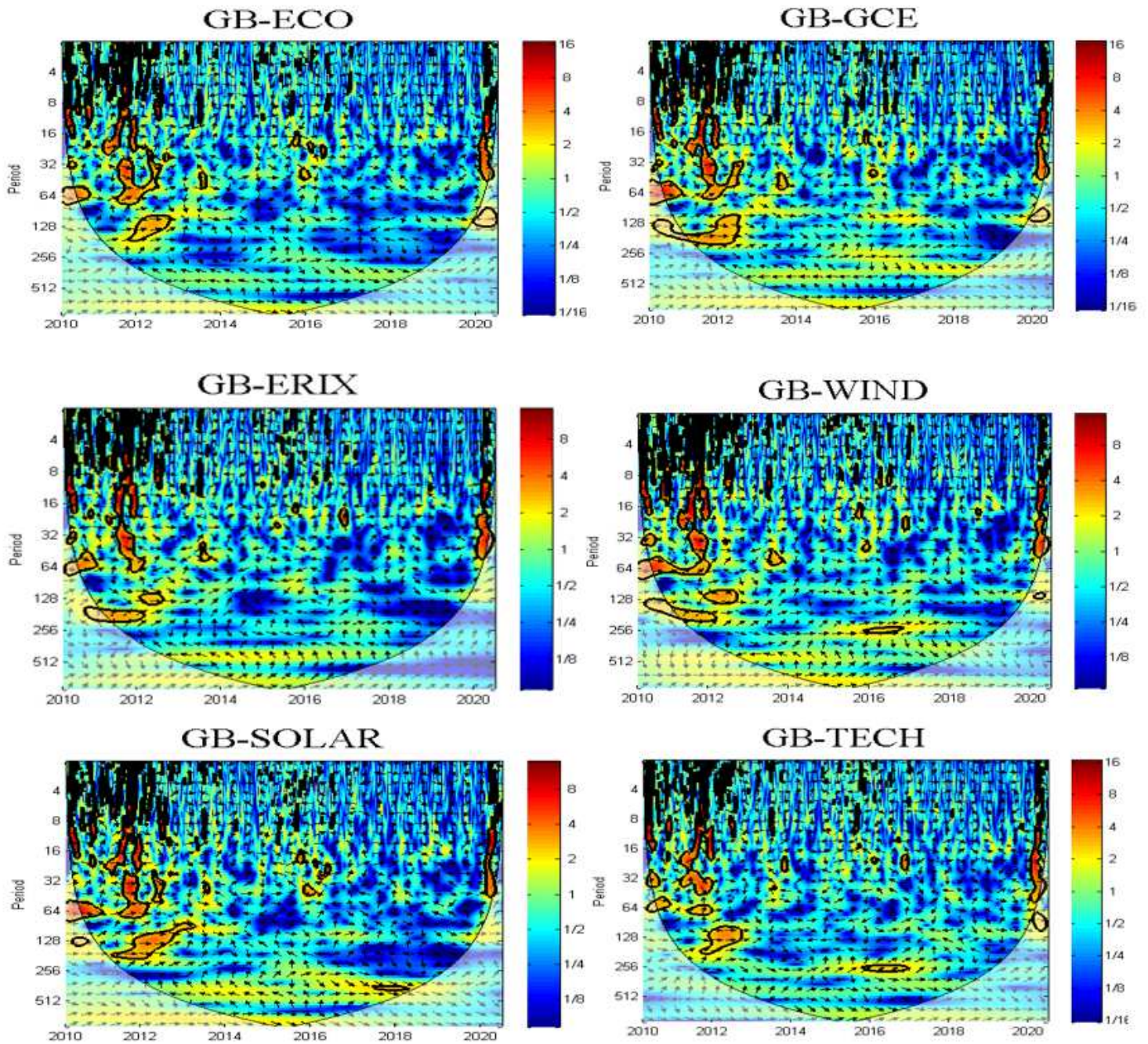


**Figure 5**

Cross-wavelet transforms for green bonds and renewable energy indices. Note: the horizontal axis presents time and the vertical axis shows frequency (days). The warmer color of the region, the higher the dependence between the pairs.

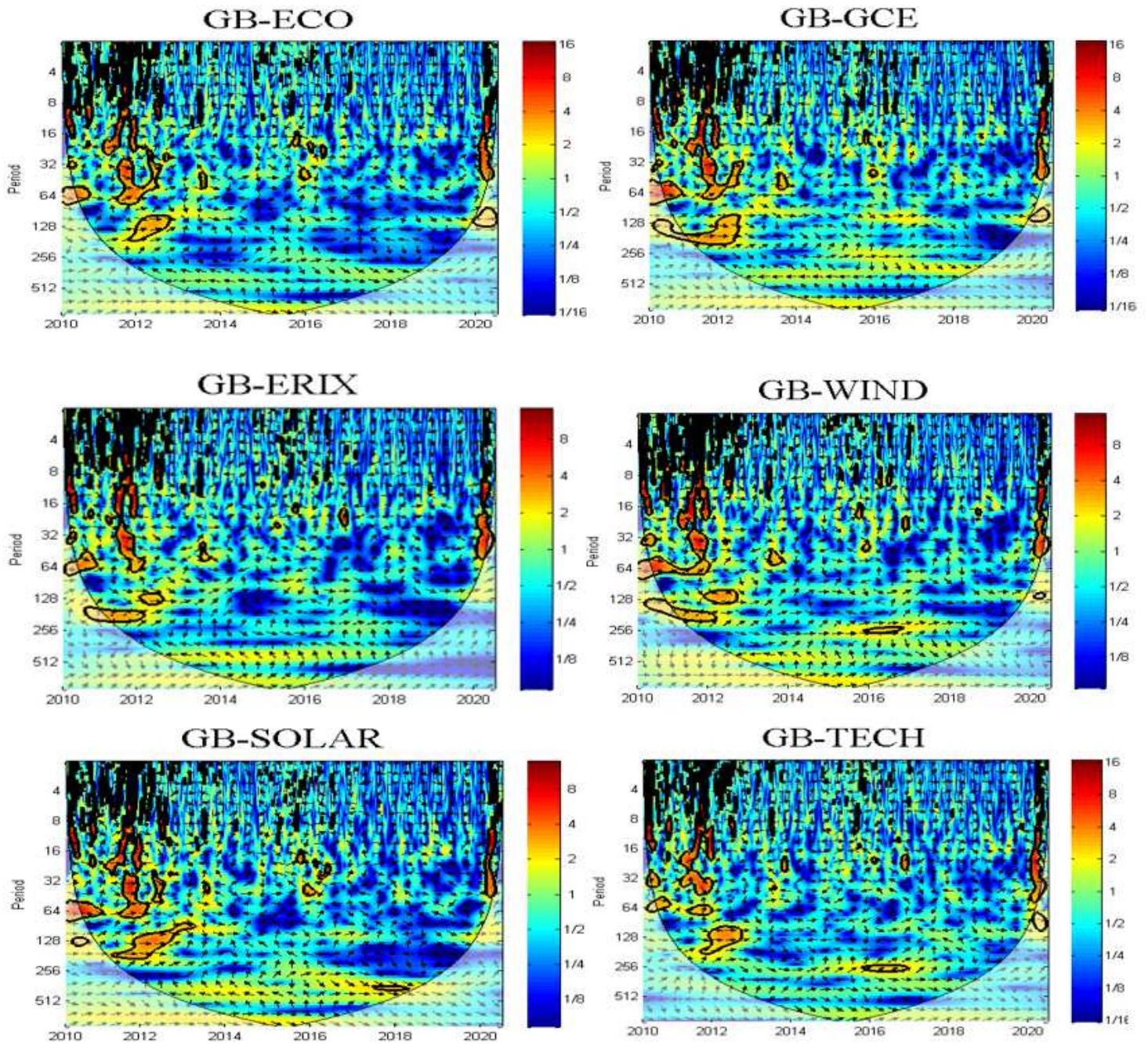


**Figure 5**

Cross-wavelet transforms for green bonds and renewable energy indices. Note: the horizontal axis presents time and the vertical axis shows frequency (days). The warmer color of the region, the higher the dependence between the pairs.

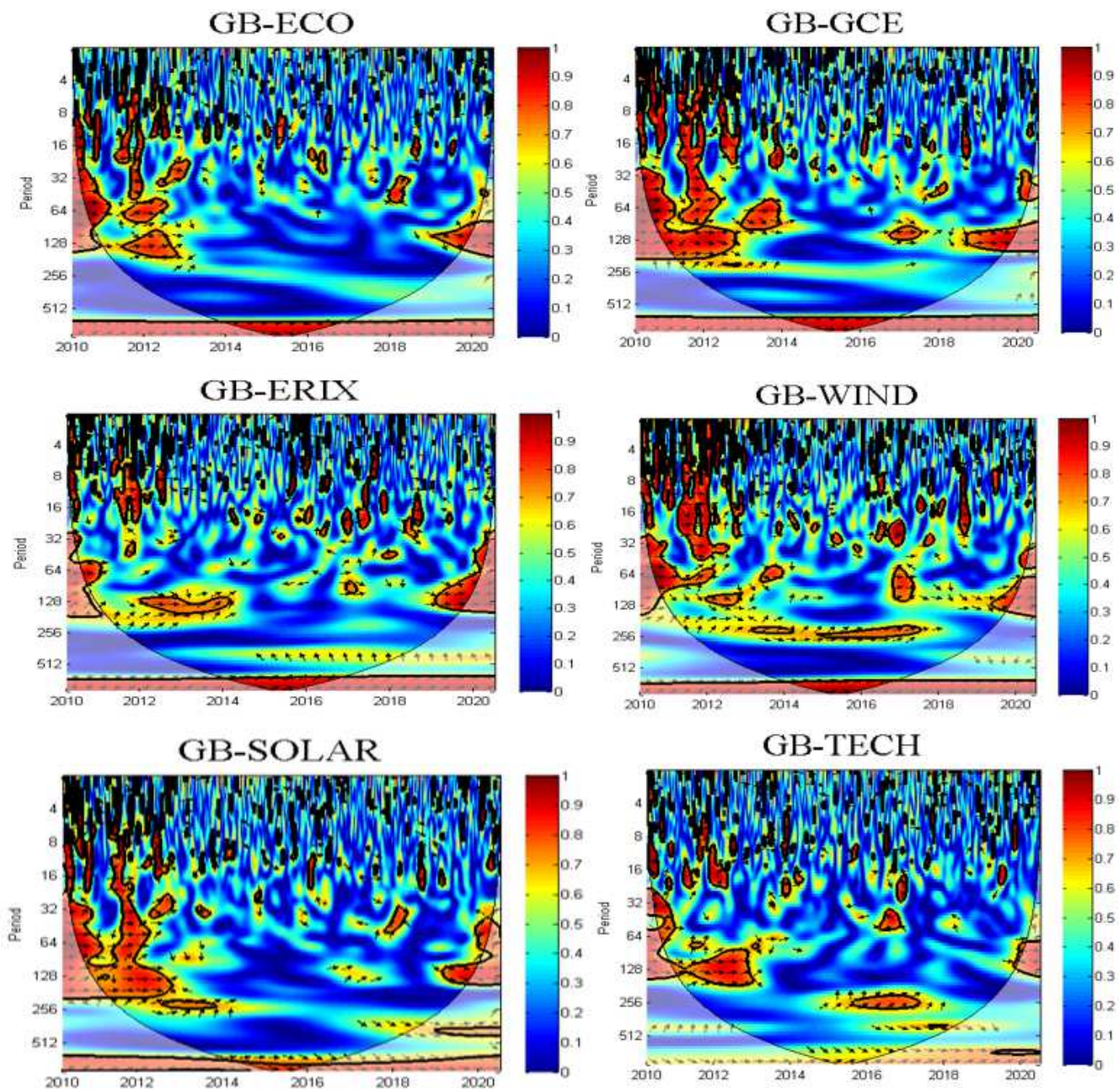


**Figure 6**

Wavelet coherence of green bonds and renewable energy pairs. Note: refer to Fig.4.

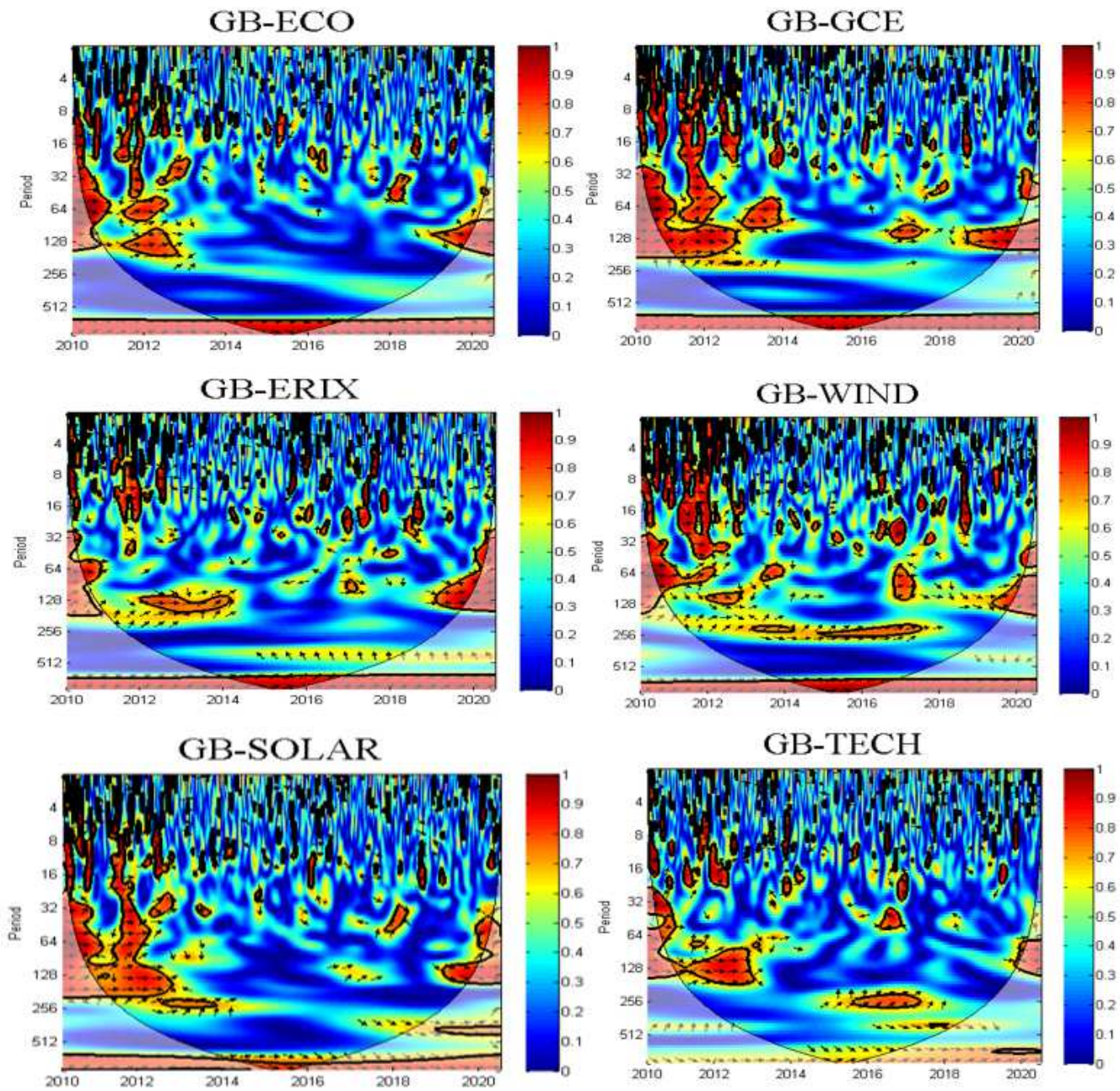


**Figure 6**

Wavelet coherence of green bonds and renewable energy pairs. Note: refer to Fig.4.

## Supplementary Files

This is a list of supplementary files associated with this preprint. Click to download.

- [data.xlsx](#)
- [data.xlsx](#)